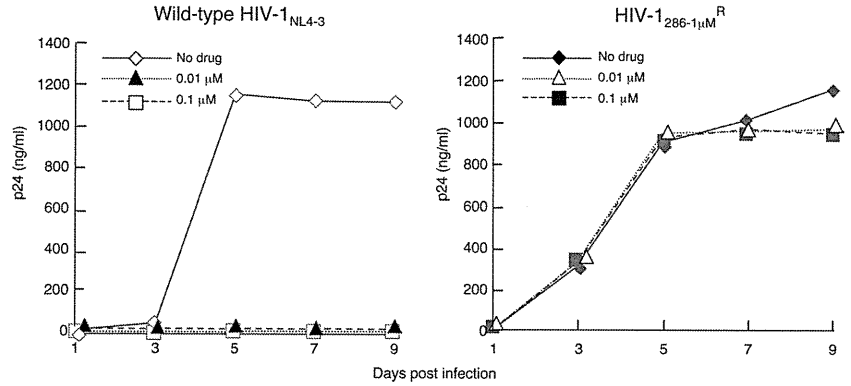

FIG. 5. Replication kinetics of GRL-286-resistant HIV-1. MT-4 cells (2.4×10^5) were exposed to an HIV-$1_{286\text{-}1\ \mu M}$ or a wild-type HIV-$1_{NL4\text{-}3}$ preparation containing 30 ng p24 in six-well culture plates for 3 h, and the MT-4 cells were divided into three fractions, each of which was cultured with or without GRL-286 (10^4 MT-4 cells/ml and drug concentrations of 0, 0.01, and 0.1 μM). The amounts of p24 were measured every 2 days for up to 9 days.

inhibitors of protease, including DRV (23). We therefore asked in the present study whether GRL-216 and GRL-286, both of which contain the *bis*-THF moiety, like DRV does, could block the dimerization of the HIV-1 protease in the system. All average $CFP^{A/B}$ ratios proved to be less than 1.0 in the presence of certain concentrations of GRL-216 and GRL-286, indicating that both compounds effectively blocked HIV-1 protease dimerization. It is thought that this protease dimerization activity, along with protease catalysis-inhibitory activity, should render GRL-216 and GRL-286 potent against diverse HIV-1 variants and cause a substantial delay in the time to the emergence of resistance to the compounds (Fig. 3).

The crystal structure of GRL-216 revealed that, as in the case of DRV (16, 25), the *bis*-THF moiety of GRL-216 forms strong hydrogen-bonding interactions with the backbones of D29 and D30 of protease and the compound has good interactions with D25 and I50, which should give GRL-216 significantly potent activity against diverse wild-type and multidrug-resistant HIV-1 strains. However, the macrocyclic ring was found to occupy more of the binding cavity of protease and form more van der Waals interactions with V82 and I84 than the corresponding isopropyl group of DRV (Fig. 7C and D). This observation should explain why HIV-1 selected with GRL-216 acquired V82I and I84V substitutions early in the selection, although GRL-216 remained fairly potent against HIV-1 variants containing these two substitutions (Table 4) (34).

Of note, if GRL-216 and GRL-286 are directly compared with DRV on the basis of the EC_{50}s alone, the compounds do not appear to possess significant advantages over DRV. However, HIV selected with the PIs examined in the present study had increased susceptibility to TPV, suggesting that combination of such mcPIs and TPV may achieve synergism. Further-

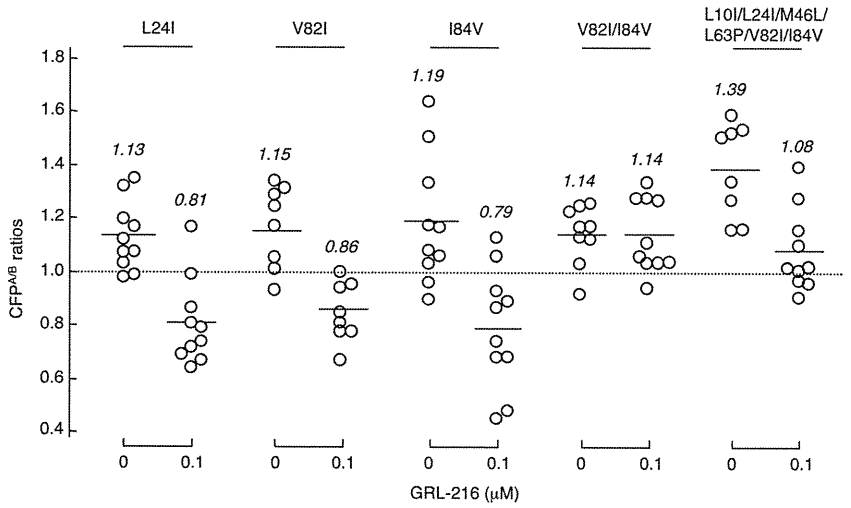

FIG. 6. GRL-216 fails to block protease dimerization with V82I and I84V substitutions. To examine whether an amino acid substitution(s) emerged upon selection of HIV-$1_{NL4\text{-}3}$ with GRL-216, recombinant clones containing the L24I, V82I, I84V, V82I/I84V, or L10I/L24I/M46L/L63P/V82I/I84V mutation(s) were generated in the setting of the FRET-based HIV-1 expression assay (23). With L24I, V82I, or I84V alone, the protease dimerization-blocking activity of 0.1 μM GRL-216 was not affected; however, with either set of the V82I/I84V or L10I/L24I/M46L/L63P/V82I/I84V substitutions, GRL-216 failed to block the dimerization.

Downloaded from http://aac.asm.org/ on February 26, 2012 by NIH Library

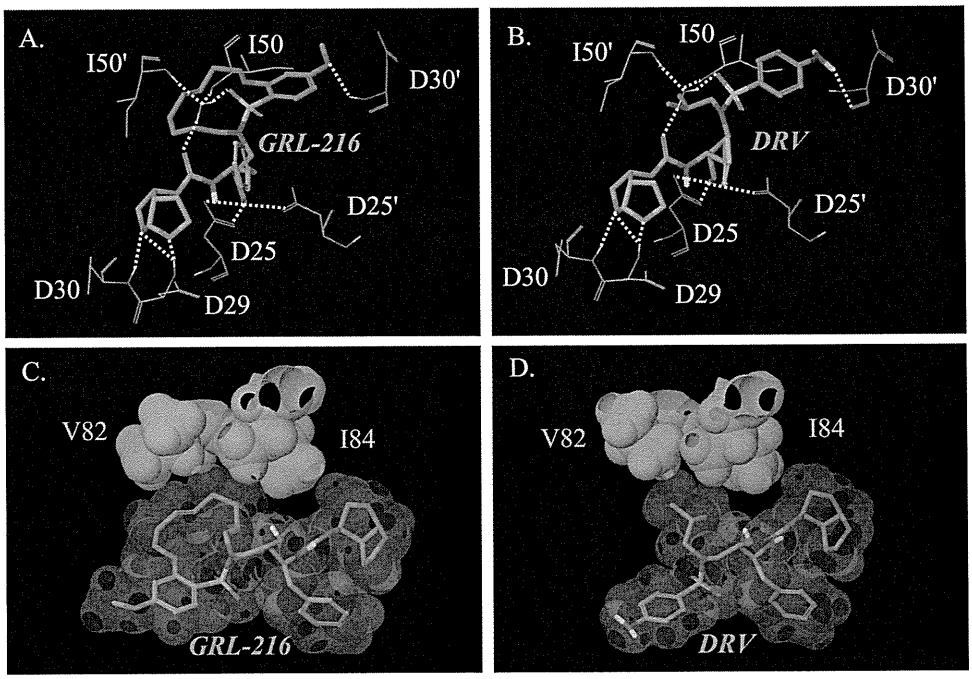

FIG. 7. Interactions of GRL-216 with HIV-1 protease compared to those of DRV. (A and B) Selected hydrogen bond interactions of GRL-216 and DRV. Both inhibitors have hydrogen bond interactions with Asp29, Asp30, Asp25, and Asp25′ and water-mediated hydrogen bond interactions with Ile50 and Ile50′ in the flap. Both inhibitors form hydrogen bond interactions with different backbone atoms of Asp30′; GRL-216 forms a hydrogen bond with the NH, while DRV forms hydrogen bonds with the oxygen of the carbonyl. (C and D) The van der Waals surfaces of GRL-216, DRV, and protease residues V82 and I84 are shown. The macrocyclic ring of GRL-216 appears to have greater van der Waals contact with V82 and I84 than the corresponding isopropyl of darunavir. All figures were generated using the Maestro (version 9.0) program (Schrödinger, LLC).

more, macrocycles represent a group of functional moieties derived from natural products, and PIs might have advantages over other PIs, including DRV.

In conclusion, the data obtained in the present study showed that GRL-216, which has dual anti-HIV-1 activity, inhibition of protease dimerization and the catalytic activity of HIV-1 protease, exerts potent activity against a wide spectrum of multidrug-resistant HIV-1 variants and that its macrocyclic moiety contributes to its increased anti-HIV-1 potency compared to that of its structurally related, *bis*-THF-containing PI DRV. The present data suggest that macrocyclic moieties may play a role in improving the anti-HIV-1 profile of PIs and in the future may contribute to the design of anti-HIV-1 compounds.

ACKNOWLEDGMENTS

This work was supported in part by the Intramural Research Program of the Center for Cancer Research, National Cancer Institute, National Institutes of Health; a grant from the National Institutes of Health (grant GM 53386 to A.K.G.); a grant from the Kumamoto University Global Center of Excellence Program, Global Education and Research Center Aiming at the Control of AIDS, supported by the Ministry of Education, Culture, Sports, Science, and Technology (Monbu-Kagakusho); a Grant-in-Aid for Scientific Research (Priority Areas) from Monbu-Kagakusho of Japan; and a Grant for Promotion of AIDS Research from the Ministry of Health, Labor and Welfare (Kosei-Rodosho) of Japan.

REFERENCES

1. **Amano, M., Y. Koh, D. Das, J. Li, S. Leschenko, Y. F. Wang, P. I. Boross, I. T. Weber, A. K. Ghosh, and H. Mitsuya.** 2007. A novel bis-tetrahydrofuranylurethane-containing nonpeptidic protease inhibitor (PI), GRL-98065, is potent against multiple-PI-resistant human immunodeficiency virus in vitro. Antimicrob. Agents Chemother. **51**:2143–2155.
2. **Bhaskaran, K., O. Hamouda, M. Sannes, F. Boufassa, A. M. Johnson, P. C. Lambert, and K. Porter.** 2008. Changes in the risk of death after HIV seroconversion compared with mortality in the general population. JAMA **300**:51–59.
3. **Carr, A.** 2003. Toxicity of antiretroviral therapy and implications for drug development. Nat. Rev. Drug Discov. **2**:624–634.
4. **Chamberlain, P. P., J. Ren, C. E. Nichols, L. Douglas, J. Lennerstrand, B. A. Larder, D. I. Stuart, and D. K. Stammers.** 2002. Crystal structures of zidovudine- or lamivudine-resistant human immunodeficiency virus type 1 reverse transcriptases containing mutations at codons 41, 184, and 215. J. Virol. **76**:10015–10019.
5. **Clavel, F., D. Guetard, F. Brun-Vezinet, S. Chamaret, M. A. Rey, M. O. Santos-Ferreira, A. G. Laurent, C. Dauguet, C. Katlama, C. Rouzioux, et al.** 1986. Isolation of a new human retrovirus from West African patients with AIDS. Science **233**:343–346.
6. **De Clercq, E.** 2010. Highlights in the discovery of antiviral drugs: a personal retrospective. J. Med. Chem. **53**:1438–1450.
7. **Doyon, L., G. Croteau, D. Thibeault, F. Poulin, L. Pilote, and D. Lamarre.** 1996. Second locus involved in human immunodeficiency virus type 1 resistance to protease inhibitors. J. Virol. **70**:3763–3769.
8. **Driggers, E. M., S. P. Hale, J. Lee, and N. K. Terrett.** 2008. The exploration of macrocycles for drug discovery—an underexploited structural class. Nat. Rev. Drug Discov. **7**:608–624.
9. **Fang, G., B. Weiser, A. Visosky, T. Moran, and H. Burger.** 1999. PCR-mediated recombination: a general method applied to construct chimeric infectious molecular clones of plasma-derived HIV-1 RNA. Nat. Med. **5**:239–242.
10. **Ferrer, E., D. Podzamczer, M. Arnedo, E. Fumero, P. McKenna, A. Rinehart, J. L. Perez, M. J. Barbera, T. Pumarola, J. M. Gatell, and F. Gudiol.** 2003. Genotype and phenotype at baseline and at failure in human immunodeficiency virus-infected antiretroviral-naive patients in a randomized trial comparing zidovudine and lamivudine plus nelfinavir or nevirapine. J. Infect. Dis. **187**:687–690.
11. **Fumero, E., and D. Podzamczer.** 2003. New patterns of HIV-1 resistance during HAART. Clin. Microbiol. Infect. **9**:1077–1084.
12. **Gatanaga, H., Y. Suzuki, H. Tsang, K. Yoshimura, M. F. Kavlick, K. Nagashima, R. J. Gorelick, S. Mardy, C. Tang, M. F. Summers, and H. Mit-**

Downloaded from http://aac.asm.org/ on February 26, 2012 by NIH Library

suya. 2002. Amino acid substitutions in Gag protein at non-cleavage sites are indispensable for the development of a high multitude of HIV-1 resistance against protease inhibitors. J. Biol. Chem. **277:**5952–5961.

13. **Ghosh, A. K., and J. H. Kim.** 2004. Stereoselective chloroacetate aldol reactions: syntheses of acetate aldol equivalents and darzens glycidic esters. Org. Lett. **6:**2725–2728.
14. **Ghosh, A. K., J. F. Kincaid, W. Cho, D. E. Walters, K. Krishnan, K. A. Hussain, Y. Koo, H. Cho, C. Rudall, L. Holland, and J. Buthod.** 1998. Potent HIV protease inhibitors incorporating high-affinity P2-ligands and (R)-(hydroxyethylamino)sulfonamide isostere. Bioorg. Med. Chem. Lett. **8:**687–690.
15. **Ghosh, A. K., K. Krishnan, D. E. Walters, W. Cho, H. Cho, Y. Koo, J. Trevino, L. Holland, and J. Buthod.** 1998. Structure based design: novel spirocyclic ethers as nonpeptidal P2-ligands for HIV protease inhibitors. Bioorg. Med. Chem. Lett. **8:**979–982.
16. **Ghosh, A. K., S. Kulkarni, D. D. Anderson, L. Hong, A. Baldridge, Y. F. Wang, A. A. Chumanevich, A. Y. Kovalevsky, Y. Tojo, M. Amano, Y. Koh, J. Tang, I. T. Weber, and H. Mitsuya.** 2009. Design, synthesis, protein-ligand X-ray structure, and biological evaluation of a series of novel macrocyclic human immunodeficiency virus-1 protease inhibitors to combat drug resistance. J. Med. Chem. **52:**7689–7705.
17. **Ghosh, A. K., S. Leshchenko, and M. Noetzel.** 2004. Stereoselective photochemical 1,3-dioxolane addition to 5-alkoxymethyl-2(5H)-furanone: synthesis of bis-tetrahydrofuranyl ligand for HIV protease inhibitor UIC-94017 (TMC-114). J. Org Chem. **69:**7822–7829.
18. **Girouard, M., K. Diallo, B. Marchand, S. McCormick, and M. Gotte.** 2003. Mutations E44D and V118I in the reverse transcriptase of HIV-1 play distinct mechanistic roles in dual resistance to AZT and 3TC. J. Biol. Chem. **278:**34403–34410.
19. **Gotte, M., D. Arion, M. A. Parniak, and M. A. Wainberg.** 2000. The M184V mutation in the reverse transcriptase of human immunodeficiency virus type 1 impairs rescue of chain-terminated DNA synthesis. J. Virol. **74:**3579–3585.
20. **Gupta, R., A. Hill, A. W. Sawyer, and D. Pillay.** 2008. Emergence of drug resistance in HIV type 1-infected patients after receipt of first-line highly active antiretroviral therapy: a systematic review of clinical trials. Clin. Infect. Dis. **47:**712–722.
21. **Hog, R.** 2008. Life expectancy of individuals on combination antiretroviral therapy in high-income countries: a collaborative analysis of 14 cohort studies. Lancet **372:**293–299.
22. **Koh, Y., D. Das, S. Leschenko, H. Nakata, H. Ogata-Aoki, M. Amano, M. Nakayama, A. K. Ghosh, and H. Mitsuya.** 2009. GRL-02031, a novel nonpeptidic protease inhibitor (PI) containing a stereochemically defined fused cyclopentanyltetrahydrofuran potent against multi-PI-resistant human immunodeficiency virus type 1 in vitro. Antimicrob. Agents Chemother. **53:**997–1006.
23. **Koh, Y., S. Matsumi, D. Das, M. Amano, D. A. Davis, J. Li, S. Leschenko, A. Baldridge, T. Shioda, R. Yarchoan, A. K. Ghosh, and H. Mitsuya.** 2007. Potent inhibition of HIV-1 replication by novel non-peptidyl small molecule inhibitors of protease dimerization. J. Biol. Chem. **282:**28709–28720.
24. **Koh, Y., H. Nakata, K. Maeda, H. Ogata, G. Bilcer, T. Devasamudram, J. F. Kincaid, P. Boross, Y. F. Wang, Y. Tie, P. Volarath, L. Gaddis, R. W. Harrison, I. T. Weber, A. K. Ghosh, and H. Mitsuya.** 2003. Novel bis-tetrahydrofuranylurethane-containing nonpeptidic protease inhibitor (PI) UIC-94017 (TMC114) with potent activity against multi-PI-resistant human immunodeficiency virus in vitro. Antimicrob. Agents Chemother. **47:**3123–3129.
25. **Kovalevsky, A. Y., A. K. Ghosh, and I. T. Weber.** 2008. Solution kinetics measurements suggest HIV-1 protease has two binding sites for darunavir and amprenavir. J. Med. Chem. **51:**6599–6603.
26. **Larder, B. A., S. D. Kemp, and P. R. Harrigan.** 1995. Potential mechanism for sustained antiretroviral efficacy of AZT-3TC combination therapy. Science **269:**696–699.
27. **Little, S. J., S. Holte, J. P. Routy, E. S. Daar, M. Markowitz, A. C. Collier, R. A. Koup, J. W. Mellors, E. Connick, B. Conway, M. Kilby, L. Wang, J. M. Whitcomb, N. S. Hellmann, and D. D. Richman.** 2002. Antiretroviral-drug resistance among patients recently infected with HIV. N. Engl. J. Med. **347:**385–394.
28. **Maeda, K., K. Yoshimura, S. Shibayama, H. Habashita, H. Tada, K. Sagawa, T. Miyakawa, M. Aoki, D. Fukushima, and H. Mitsuya.** 2001. Novel low molecular weight spirodiketopiperazine derivatives potently inhibit R5 HIV-1 infection through their antagonistic effects on CCR5. J. Biol. Chem. **276:**35194–35200.
29. **Mitsuya, H., and J. Erickson.** 1999. Discovery and development of antiretroviral therapeutics for HIV infection, p. 751–780. *In* T. C. Merigan, J. G. Bartlet, and D. Bolognesi (ed.), Textbook of AIDS medicine. The Williams & Wilkins Co., Baltimore, MD.
30. **Murphy, E. L., A. C. Collier, L. A. Kalish, S. F. Assmann, M. F. Para, T. P. Flanigan, P. N. Kumar, L. Mintz, F. R. Wallach, and G. J. Nemo.** 2001. Highly active antiretroviral therapy decreases mortality and morbidity in patients with advanced HIV disease. Ann. Intern. Med. **135:**17–26.
31. **Naeger, L. K., and K. A. Struble.** 2007. Food and Drug Administration analysis of tipranavir clinical resistance in HIV-1-infected treatment-experienced patients. AIDS **21:**179–185.
32. **Shirasaka, T., R. Yarchoan, M. C. O'Brien, R. N. Husson, B. D. Anderson, E. Kojima, T. Shimada, S. Broder, and H. Mitsuya.** 1993. Changes in drug sensitivity of human immunodeficiency virus type 1 during therapy with azidothymidine, dideoxycytidine, and dideoxyinosine: an in vitro comparative study. Proc. Natl. Acad. Sci. U. S. A. **90:**562–566.
33. **Siliciano, J. D., and R. F. Siliciano.** 2004. A long-term latent reservoir for HIV-1: discovery and clinical implications. J. Antimicrob. Chemother. **54:**6–9.
34. **Tie, Y., P. I. Boross, Y. F. Wang, L. Gaddis, A. K. Hussain, S. Leshchenko, A. K. Ghosh, J. M. Louis, R. W. Harrison, and I. T. Weber.** 2004. High resolution crystal structures of HIV-1 protease with a potent non-peptide inhibitor (UIC-94017) active against multi-drug-resistant clinical strains. J. Mol. Biol. **338:**341–352.
35. **Walensky, R. P., A. D. Paltiel, E. Losina, L. M. Mercincavage, B. R. Schackman, P. E. Sax, M. C. Weinstein, and K. A. Freedberg.** 2006. The survival benefits of AIDS treatment in the United States. J. Infect. Dis. **194:**11–19.
36. **Yoshimura, K., R. Kato, M. F. Kavlick, A. Nguyen, V. Maroun, K. Maeda, K. A. Hussain, A. K. Ghosh, S. V. Gulnik, J. W. Erickson, and H. Mitsuya.** 2002. A potent human immunodeficiency virus type 1 protease inhibitor, UIC-94003 (TMC-126), and selection of a novel (A28S) mutation in the protease active site. J. Virol. **76:**1349–1358.
37. **Yoshimura, K., R. Kato, K. Yusa, M. F. Kavlick, V. Maroun, A. Nguyen, T. Mimoto, T. Ueno, M. Shintani, J. Falloon, H. Masur, H. Hayashi, J. Erickson, and H. Mitsuya.** 1999. JE-2147: a dipeptide protease inhibitor (PI) that potently inhibits multi-PI-resistant HIV-1. Proc. Natl. Acad. Sci. U. S. A. **96:**8675–8680.

Downloaded from http://aac.asm.org/ on February 26, 2012 by NIH Library

Bioorganic & Medicinal Chemistry Letters 20 (2010) 1241–1246

Contents lists available at ScienceDirect

Bioorganic & Medicinal Chemistry Letters

journal homepage: www.elsevier.com/locate/bmcl

Synthesis and biological evaluation of novel allophenylnorstatine-based HIV-1 protease inhibitors incorporating high affinity P2-ligands

Arun K. Ghosh [a,*], Sandra Gemma [a], Elena Simoni [a], Abigail Baldridge [a], D. Eric Walters [b], Kazuhiko Ide [c], Yasushi Tojo [c], Yasuhiro Koh [c], Masayuki Amano [c], Hiroaki Mitsuya [c,d]

[a] Departments of Chemistry and Medicinal Chemistry, Purdue University, West Lafayette, IN 47907, United States
[b] Departments of Biochemistry and Molecular Biology, Rosalind Franklin University of Medicine and Science, North Chicago, IL 60064, United States
[c] Departments of Hematology and Infectious Diseases, Kumamoto University School of Medicine, Kumamoto 860-8556, Japan
[d] Experimental Retrovirology Section, HIV and AIDS Malignancy Branch, National Cancer Institute, Bethesda, MD 20892, United States

ARTICLE INFO

Article history:
Received 19 October 2009
Revised 20 November 2009
Accepted 23 November 2009
Available online 5 December 2009

Keywords:
HIV protease
Inhibitors
Darunavir
Allophenylnorstatine
Design
Synthesis

ABSTRACT

A series of stereochemically defined cyclic ethers as P2-ligands were incorporated in an allophenylnorstatine-based isostere to provide a new series of HIV-1 protease inhibitors. Inhibitors **3b** and **3c**, containing conformationally constrained cyclic ethers, displayed impressive enzymatic and antiviral properties and represent promising lead compounds for further optimization.

© 2009 Elsevier Ltd. All rights reserved.

The introduction of protease inhibitors into highly active antiretroviral treatment (HAART) regimens with reverse transcriptase inhibitors represented a major breakthrough in AIDS chemotherapy.[1] This combination therapy has significantly increased life expectancy, and greatly improved the course of HIV management. Therapeutic inhibition of HIV-1 protease leads to morphologically immature and noninfectious viral particles.[2] However, under the selective pressure of chemotherapeutics, rapid adaptation of viral enzymes generates strains resistant to one or more antiviral agents.[3] As a consequence, a growing number of HIV/AIDS patients harbor multidrug-resistant HIV strains. There is ample evidence that such strains can be readily transmitted.[4] Therefore, one of the major current therapeutic objectives has been to develop novel protease inhibitors (PIs) with broad-spectrum activity against multidrug-resistant HIV-1 variants. In our continuing interest in developing concepts and strategies to combat drug-resistance, we have reported a series of novel PIs including Darunavir, TMC-126, GRL-06579, and GRL-02031.[5–8] These inhibitors have shown exceedingly potent enzyme inhibitory and antiviral activity as well as exceptional broad spectrum activity against highly cross-resistant mutants. Darunavir, which incorporates a (*R*)-(hydroxymethyl)-sulfonamide isostere and a stereochemically defined bis-tetrahydrofuran (bis-THF) as the P2-ligand, was initially approved for the treatment of patients with drug-resistant HIV and more recently, it has been approved for all HIV/AIDS patients including pediatrics[9] (Fig. 1).

Darunavir was designed based upon the 'backbone binding' concept developed in our laboratories. Darunavir-bound X-ray structure revealed extensive hydrogen bonding with the protease backbone throughout the enzyme active site.[10] The P2-bis-THF ligand is responsible for its superior drug-resistance properties. The bis-THF ligand has been documented as a privileged ligand for the S2-subsite. Incorporation of this ligand into other transition-state isosteres also resulted in significant potency enhancement.[11] Besides 3(*S*)-THF, and [3*aS*,5*S*,6*R*]-bis-THF, we have designed a number of other novel cyclic ether-based high affinity ligands. Incorporation of these ligands in (*R*)-(hydroxyethyl)-sulfonamide isosteres provided PIs with excellent potency and drug-resistance properties.[6–8] We then investigated the potential of these structure-based designed P2-ligands in a KNI-764-derived isostere designed by Mimoto and coworkers.[12] This PI incorporates an allophenylnorstatine isostere. Interestingly, KNI-764 has maintained good activity against HIV-1 clinical strains resistant to several FDA-approved PIs. The flexible *N*-(2-methyl benzyl) amide P2′-ligand may have been responsible for its activity against drug-resistant HIV-1 strains as the flexible chain allows better adaptability to mutations.[12,13] The bis-THF and other structure-based designed P2-ligands, make several critical

* Corresponding author. Tel.: +1 765 494 5323; fax: +1 765 496 1612.
E-mail address: akghosh@purdue.edu (A.K. Ghosh).

0960-894X/$ - see front matter © 2009 Elsevier Ltd. All rights reserved.
doi:10.1016/j.bmcl.2009.11.123

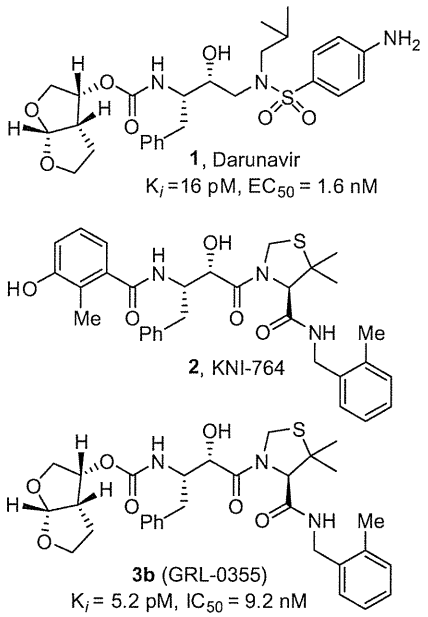

Figure 1. Structures of inhibitors **1**, **2**, and **3b**.

hydrogen bonds with the protein backbone, particularly with Asp-29 and Asp-30 NH's.[11] Therefore, incorporation of these ligands into the KNI-764-derived isostere, may lead to novel PIs with improved potency and efficacy against multidrug-resistant HIV-1 variants. Furthermore, substitution of the P2-phenolic derivative in KNI-764 with a cyclic ether-based ligand could result in improved metabolic stability and pharmacological properties since phenol glucuronide is readily formed when KNI-764 is exposed to human hepatocytes in vitro.[12]

The synthesis of target compounds **3a–e** was accomplished as described in Scheme 1. Our synthetic plan for carboxylic acid **7** (Scheme 1) involved the preparation of the key intermediate **5** through two different synthetic pathways. In the first approach, known optically active azidodiol **4**[14] was first hydrogenated in the presence of Boc_2O. The resulting diol was converted to **5** by selective acylation of the primary alcohol with acetic anhydride in the presence of pyridine and a catalytic amount of DMAP at 0 °C for 4 h to provide **5** in 77% overall yield. As an alternative approach, commercially available optically active epoxide **6** was exposed to lithium acetate, formed in situ from lithium carbonate and acetic acid in DMF. This resulted in the regioselective opening[15] of the epoxide ring and afforded compound **5** in 62% yield. The alcohol **5** thus obtained was protected as the corresponding acetonide by treatment with 2-methoxypropene in the presence of a catalytic amount of CSA. The acetate group was subsequently hydrolyzed in the presence of potassium carbonate in methanol to afford the corresponding alcohol. This was subjected to an oxidation reaction using ruthenium chloride hydrate and sodium periodate in a mixture of aqueous acetonitrile and CCl_4 at 23 °C for 10 h. This resulted in the formation of the target carboxylic acid **7** in 61% yield. Amide **9a** was prepared by activation of carboxylic acid **7** into the corresponding mixed anhydride by treatment with isobutylchloroformate followed by reaction with amine **8a**.[16,17]

Synthesis of various inhibitors was carried out as shown in Scheme 2. Deprotection of the Boc and acetonide groups was carried out by exposure of **9** to a 1 M solution of hydrochloric acid in methanol at 23 °C for 8 h. This provided amine **10** in quantitative

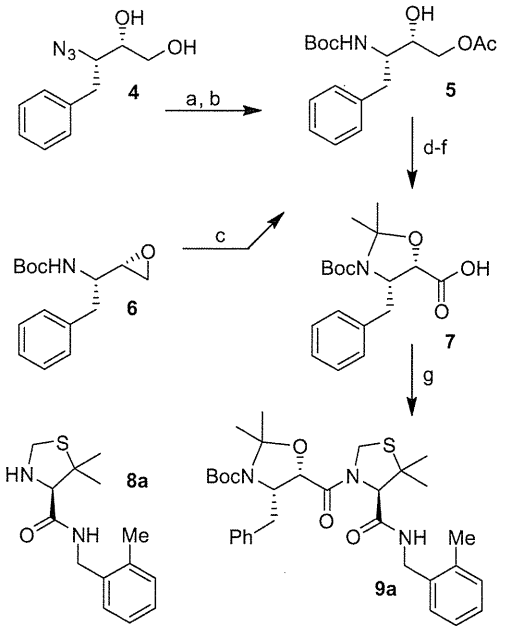

Scheme 1. Reagents: (a) H_2, Pd/C, Boc_2O, EtOAc; (b) Ac_2O, Pyr, DMAP; (c) $LiCO_3$, AcOH, DMF; (d) 2-methoxypropene, CSA, DCM; (e) K_2CO_3, MeOH; (f) $RuCl_3$, $NaIO_4$, CCl_4–MeCN–H_2O (2:2:3); (g) *N*-methylmorpholine, *i*BuOCOCl, **8a**, THF.

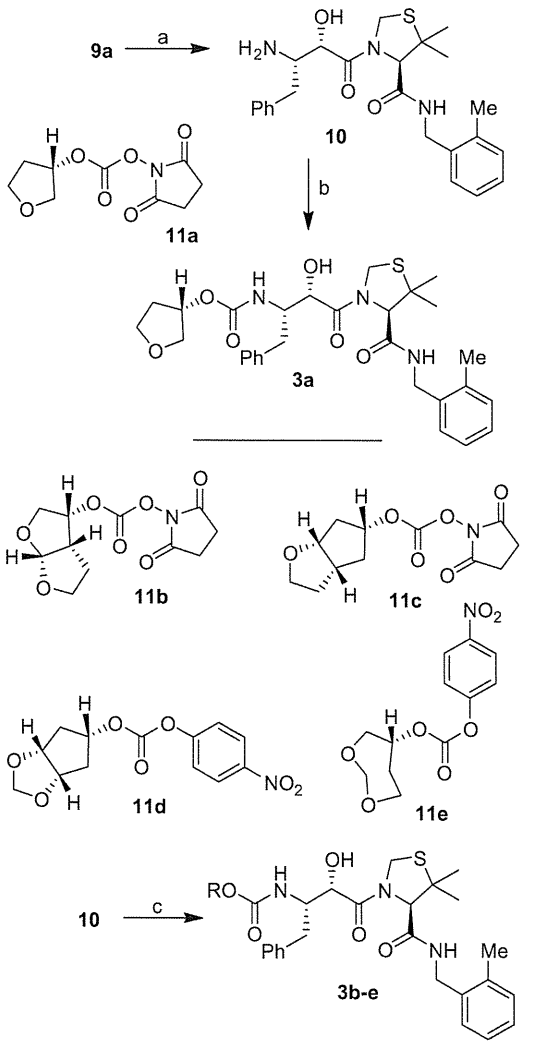

Scheme 2. Reagents: (a) 1 M HCl, MeOH; (b) **11a**, Et_3N, CH_2Cl_2; (c) **11b,c**, Et_3N, CH_2Cl_2; or, **11d,e**, DIPEA, THF.

yield. Reaction of **11a** with amine **10** in CH_2Cl_2 in the presence of Et_3N at 23 °C for 6 h, provided inhibitor **3a** in 62% yield. The 3(*S*)-tetrahydrofuranyl carbonate **11a** was prepared as described previously.[18] Similarly, allophenylnorstatine-based inhibitors **3b–e** were synthesized. As shown, carbonates **11b**,[19] **11c**,[7] and **11d–e**[19] were prepared as previously described. Reaction of these carbonates with amine **10** furnished the desired inhibitors **3b–e** in 45–62% yield.

The syntheses of inhibitors **14a,b** and **16a–c** were carried out as shown in Scheme 3. Inhibitors **14a,b**, containing hydroxyethylamine isostere were prepared by opening epoxide **6** with amine **8a** in the presence of lithium perchlorate in diethyl ether at 23 °C for 5 h to provide amino alcohol **12** in 64% yield. Removal of the Boc-group by exposure to 1 M HCl in MeOH at 23 °C for 12 h afforded amine **13**. Reactions of amine **13** with activated carbonates **11a** and **11b** afforded urethane **14a** and **14b** in 44% and 59% yields, respectively. For the synthesis of inhibitors **16a–c**, commercially available (*R*)-5,5-dimethyl-thiazolidine-4-carboxylic acid was protected as its Boc-derivative. The resulting acid was coupled with amines **15a–c** in the presence of DCC and DMAP in CH_2Cl_2 to provide the corresponding amides. Removal of the Boc-group by exposure to 30% trifluoroacetic acid afforded **8b–d**. Coupling of these amines with acid **7** as described in Scheme 1, provided the corresponding products **9b–d**. Removal of Boc-group and reactions of the resulting amines with activated carbonate **11b** furnished inhibitors **16a–c** in good yields (55–60%).

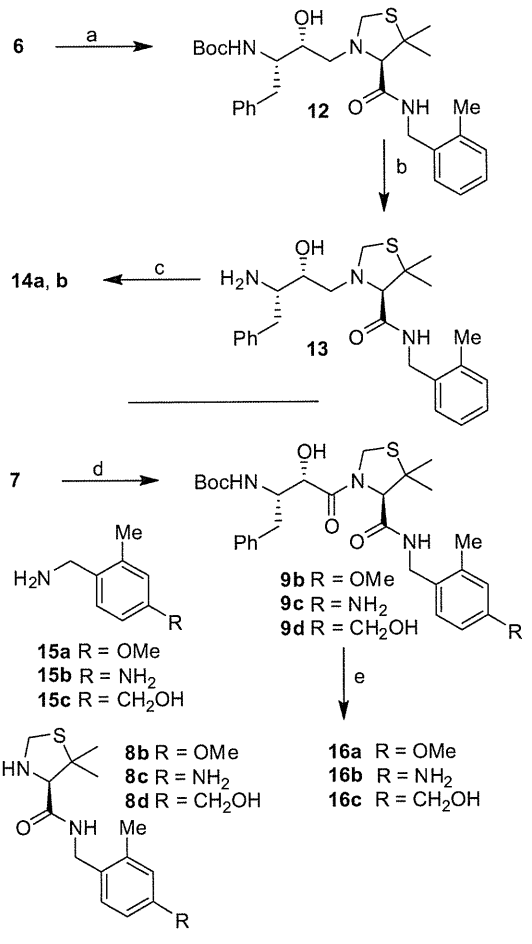

Scheme 3. Reagents: (a) **8a**, $Li(ClO_4)$, Et_2O; (b) CF_3CO_2H, CH_2Cl_2; (c) **11a** or, **11b**, Et_3N, CH_2Cl_2; (d) *N*-methylmorpholine, *isobutylchloroformate*, **8b-d**, THF; (e) CF_3CO_2H, CH_2Cl_2, then **11b**, Et_3N, CH_2Cl_2.

Inhibitors **3a–e** were first evaluated in enzyme inhibitory assay utilizing the protocol described by Toth and Marshall.[20] Compounds that showed potent enzymatic K_i values were then further evaluated in antiviral assay. The inhibitor structure and potency are shown in Table 1. As shown, incorporation of a stereochemically defined 3(*S*)-tetrahydrofuran ring as the P2-ligand provided inhibitor **3a**, which displayed an enzyme inhibitory potency of 0.2 nM and antiviral IC_{50} value of 20 nM. The corresponding derivative **14a** with a hydroxyethylamine isostere exhibited over 400-fold reduction in enzyme inhibitory activity. Introduction of a stereochemically defined bis-THF as the P2-ligand, resulted in inhibitor **3b**, which displayed over 40-fold potency enhancement with respect to **3a**. Inhibitor **3b** displayed a K_i of 5.2 pM in the enzyme inhibitory assay. Furthermore, compound **3b** has shown an impressive antiviral activity with an IC_{50} value of 9 nM. Inhibitor **14b** with hydroxyethylamine isostere is significantly less potent than the corresponding norstatine-derived inhibitor **3b**. Inhibitor **3c** with a (3a*S*, 5*R*, 6a*R*)-5-hydroxy-hexahydrocyclopenta[*b*]furan as the P2-ligand has displayed excellent inhibitory activity, and particularly, antiviral activity, showing an IC_{50} value of 13 nM. Other structure-based designed ligands in inhibitors **3d** and **3e** have shown subnanomolar enzyme inhibitory activity. However, inhibitor **3b** with a bis-THF ligand has shown the most impressive activity.

To obtain molecular insight into the possible ligand-binding site interactions, we have created energy-minimized models of a number of inhibitors based upon protein-ligand X-ray structure of KNI-764 (**2**).[21] An overlayed model of **3b** with the X-ray structure of **2**-bound HIV-1 protease is shown in Figure 2. This model for inhibitor **3b** was created from the X-ray crystal structure of KNI-764 (**2**)-bound HIV-1 protease (KNI-764, pdb code 1MSM[21]) and the X-ray crystal structure of darunavir (pdb code 2IEN[22]), by combining the P2-end of the darunavir structure with the P2′-end of the KNI-764 structure, followed by 1000 cycles of energy minimization. It appears that both oxygens of the bis-THF ligand are suitably located to form hydrogen bonds with the backbone atoms of Asp-29 and Asp-30 NH's, similar to darunavir-bound HIV-1 protease.[10] Furthermore, the KNI-764-X-ray structure-derived model of **3b** suggested that the incorporation of appropriate substituents on the phenyl ring could interact with Asp-29′ and Asp-30′ in the S2′-subsite. In particular, it appears that a 4-hydroxymethyl substituent on the P2′-phenyl ring could conceivably interact with backbone Asp-30′ NH in the S2′-subsite. Other substituents such as a methoxy group or an amine functionality also appears to be within proximity to Asp-29′ and Asp-30′ backbone NHs. Based upon these speculations, we incorporated *p*-MeO, *p*-NH_2 and *p*-CH_2OH substituents on the P2′-phenyl ring of inhibitor **3b**. As shown in Table 1, neither *p*-MeO nor *p*-NH_2 groups improved enzyme inhibitory potency compared to inhibitor **3b**. Of particular note, compound **16a**, displayed a good antiviral potency, possibly suggesting a better penetration through the cell membrane. Inhibitor **16c** with a hydroxymethyl substituent showed sub-nanomolar enzyme inhibitory potency but its antiviral activity was moderate compared to unsubstituted derivative **3b**. As it turned out, inhibitor **3b** is the most potent inhibitor in the series. We subsequently examined its activity against a clinical wild-type X_4-HIV-1 isolate (HIV-$1_{ERS104pre}$) along with various multidrug-resistant clinical X_4- and R_5- HIV-1 isolates using PBMCs as target cells.[5b] As can be seen in Table 2, the potency of **3b** against HIV-$1_{ER104pre}$ (IC_{50} = 31 nM) was comparable to the FDA approved PI, amprenavir with an IC_{50} value of 45 nM. Darunavir and atazanavir on the other hand, are significantly more potent with IC_{50} values of 5 nM and 3 nM, respectively. Inhibitor **3b**, while less potent than darunavir, maintained 5-fold or better potency over amprenavir against HIV-$1_{MDR/C}$, HIV-$1_{MDR/G}$, HIV-$1_{MDR/TM}$ and HIV-$1_{MDR/MM}$. It maintained over a 2-fold potency against HIV-$1_{MDR/JSL}$. In fact, inhibitor **3b** maintained comparable potency to atazanavir against all

Table 1
Enzymatic inhibitory and antiviral activity of allophenylnorstatine-derived inhibitors

Entry	Inhibitor	K_i (nM)	IC_{50}[a,b] (μM)
1	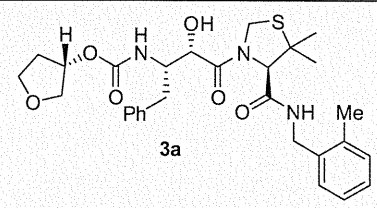 **3a**	0.21	0.02
2	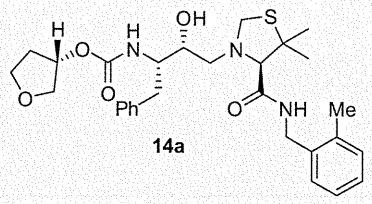 **14a**	86.2	nt
3	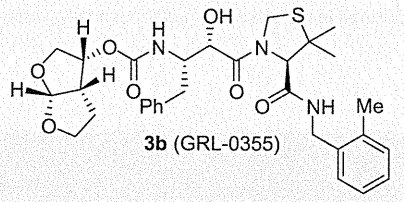 **3b** (GRL-0355)	0.0052	0.009
4	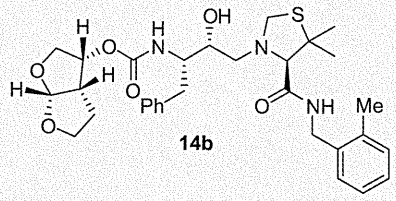 **14b**	2.6	nt
5	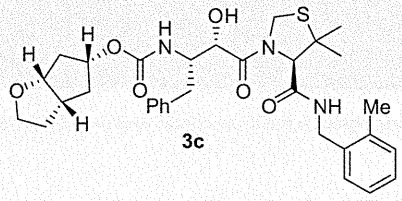 **3c**	0.29	0.013
6	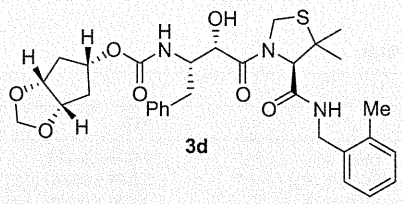 **3d**	0.65	nt
7	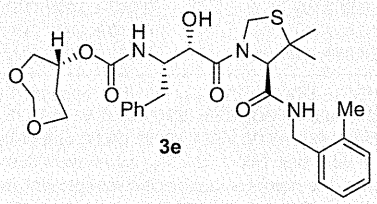 **3e**	0.78	nt
8	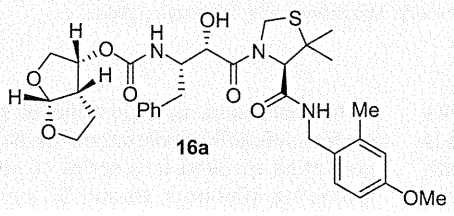 **16a**	2.03	0.051

Table 1 (*continued*)

Entry	Inhibitor	K_i (nM)	IC_{50}[a,b] (μM)
9	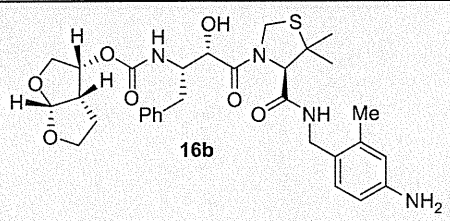 **16b**	1.01	0.53
10	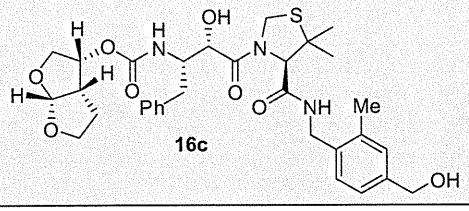 **16c**	0.31	0.23

[a] Values are means of at least three experiments.
[b] Human lymphoid (MT-2) cells were exposed to 100 $TCID_{50}$ values of HIV-1_{LAI} and cultured in the presence of each PI, and IC_{50} values were determined using MTT assay. Darunavir exhibited K_i = 16 pM, IC_{50} = 1.6 nM.

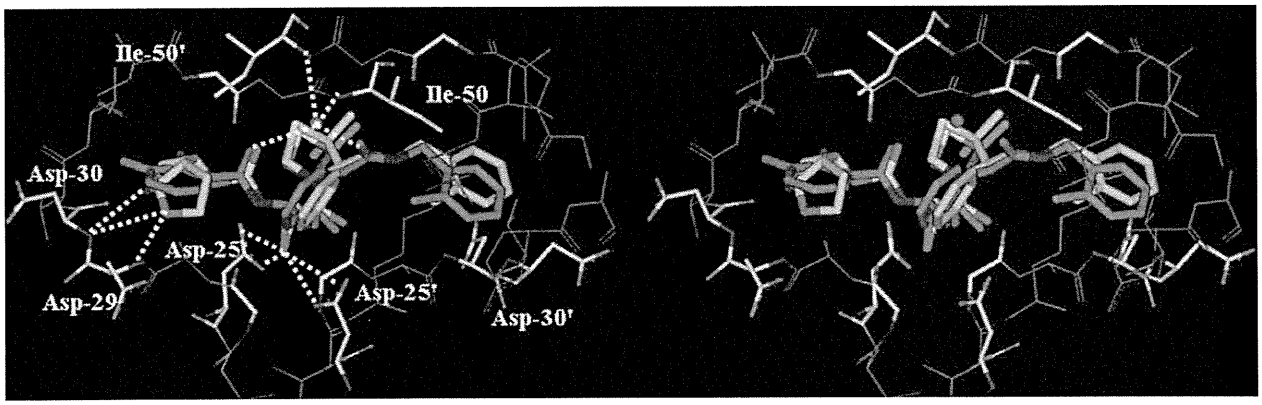

Figure 2. Structure of inhibitor **3b**, modeled into the active site of HIV-1 protease, superimposed on the X-ray crystal structure of KNI-764. Inhibitor **3b** carbons are shown in green and KNI-764 carbons are shown in magenta.

Table 2
Antiviral activity of **3b** (GRL-0355) against multidrug-resistant clinical isolates in PHA-PBMs.

Virus	IC_{50} (μM)			
	3b (GRL-0355)	APV	ATV	DRV
HIV-$1_{ERS104pre}$ (wild-type: X4)	0.031 ± 0.002	0.045 ± 0.014	0.003 ± 0.003	0.005 ± 0.001
HIV-$1_{MDR/C}$ (X4)	0.061 ± 0.005 (2)	0.346 ± 0.071 (8)	0.045 ± 0.026 (15)	0.010 ± 0.006 (2)
HIV-$1_{MDR/G}$ (X4)	0.029 ± 0.002 (1)	0.392 ± 0.037 (9)	0.029 ± 0.020 (10)	0.019 ± 0.005 (4)
HIV-$1_{MDR/TM}$ (X4)	0.064 ± 0.032 (2)	0.406 ± 0.082 (9)	0.047 ± 0.009 (16)	0.007 ± 0.003 (1)
HIV-$1_{MDR/MM}$ (R5)	0.042 ± 0.001 (1)	0.313 ± 0.022 (7)	0.040 ± 0.002 (13)	0.027 ± 0.008 (5)
HIV-$1_{MDR/JSL}$ (R5)	0.235 ± 0.032 (8)	0.531 ± 0.069 (12)	0.635 ± 0.065 (212)	0.028 ± 0.008 (6)

The amino acid substitutions identified in the protease-encoding region of HIV-$1_{ERS104pre}$, HIV-1_C, HIV-1_G, HIV-1_{MM}, HIV-1_{JSL} compared to the consensus type B sequence cited from the Los Alamos database include L63P; L10I, I15V, K20R, L24I, M36I, M46L, I54V, I62V, L63P, K70Q,V82A, L89M; L10I, V11I, T12E, I15V, L19I, R41K, M46L, L63P, A71T, V82A, L90M; L10I, K14R, R41K, M46L, I54V, L63P, A71V, V82A, L90M; L10I, K43T, M46L, I54V, L63P, A71V, V82A, L90M, Q92K; and L10I, L24I, I33F, E35D, M36I, N37S, M46L, I54V, R57K, I62V, L63P, A71V, G73S, V82A, respectively. HIV-$1_{ERS104pre}$ served as a source of wild-type HIV-1. The IC_{50} values were determined by using PHA-PBMs as target cells and the inhibition of p24 Gag protein production by each drug was used as an endpoint. The numbers in parentheses represent the fold changes of IC_{50} values for each isolate compared to the IC_{50} values for wild-type HIV-$1_{ERS104pre}$. All assays were conducted in duplicate, and the data shown represent mean values (±1 standard deviations) derived from the results of two or three independent experiments. Amprenavir = APV; Atazanavir = ATV; Darunavir = DRV.

multidrug-resistant clinical isolates tested. The reason for its impressive potency against multidrug-resistant clinical isolates is possibly due to its ability to make extensive hydrogen-bonds with the protease backbone in the S2 subsite and its ability to fill in the hydrophobic pockets in the S1′–S2′ subsites effectively.

In conclusion, incorporation of stereochemically defined and conformationally constrained cyclic ethers into the allophenylnorstatine resulted in a series of potent protease inhibitors. The promising inhibitors **3b** and **3c** are currently being subjected to further in-depth biological studies. Design and synthesis of new

classes of inhibitors based upon above molecular insight are currently ongoing in our laboratories.

Acknowledgement

The financial support of this work is provided by the National Institute of Health (GM 83356).

References and notes

1. Sepkowitz, K. A. *N. Eng. J. Med.* **2001**, *344*, 1764–1772.
2. Kohl, N. E.; Emini, E. A.; Schleif, W. A.; Davis, L. J.; Heimbach, J. C.; Dixon, R. A. F.; Scolnick, E. M.; Sigal, I. S. *Proc. Natl. Acad. Sci. U.S.A.* **1988**, *85*, 4686–4690.
3. (a) Pillay, D.; Bhaskaran, K.; Jurriaans, S.; Prins, M.; Masquelier, B.; Dabis, F.; Gifford, R.; Nielsen, C.; Pedersen, C.; Balotta, C.; Rezza, G.; Ortiz, M.; de Mendoza, C.; Kücherer, C.; Poggensee, G.; Gill, J.; Porter, K. *AIDS* **2006**, *20*, 21–28; (b) Grabar, S.; Pradier, C.; Le Corfec, E.; Lancar, R.; Allavena, C.; Bentata, M.; Berlureau, P.; Dupont, C.; Fabbro-Peray, P.; Poizot-Martin, I.; Costagliola, D. *AIDS* **2000**, *14*, 141–149.
4. Wainberg, M. A.; Friedland, G. *JAMA* **1998**, *279*, 1977–1983.
5. (a) Ghosh, A. K.; Kincaid, J. F.; Cho, W.; Walters, D. E.; Krishnan, K.; Hussain, K. A.; Koo, Y.; Cho, H.; Rudall, C.; Holland, L.; Buthod, J. *Bioorg. Med. Chem. Lett.* **1998**, *8*, 687–690; (b) Koh, Y.; Maeda, K.; Ogata, H.; Bilcer, G.; Devasamudram, T.; Kincaid, J. F.; Boross, P.; Wang, Y.-F.; Tie, Y.; Volarath, P.; Gaddis, L.; Louis, J. M.; Harrison, R. W.; Weber, I. T.; Ghosh, A. K.; Mitsuya, H. *Antimicrob. Agents Chemother.* **2003**, *47*, 3123–3129; (c) Ghosh, A. K.; Pretzer, E.; Cho, H.; Hussain, K. A.; Duzgunes, N. *Antiviral Res.* **2002**, *54*, 29–36.
6. Yoshimura, K.; Kato, R.; Kavlick, M. F.; Nguyen, A.; Maroun, V.; Maeda, K.; Hussain, K. A.; Ghosh, A. K.; Gulnik, S. V.; Erickson, J. W.; Mitsuya, H. *J. Virol.* **2002**, *76*, 1349–1358.
7. Ghosh, A. K.; Sridhar, P. R.; Leshchenko, S.; Hussain, A. K.; Li, J.; Kovalevsky, A. Y.; Walters, D. E.; Wedekind, J. K.; Grum-Tokars, V.; Das, D.; Koh, Y.; Maeda, K.; Gatanaga, H.; Weber, I. T.; Mitsuya, H. *J. Med. Chem.* **2006**, *49*, 5252.
8. Koh, Y.; Das, D.; Leshchenko, S.; Nakata, H.; Ogata-Aoki, H.; Amano, M.; Nakayama, M.; Ghosh, A. K.; Mitsuya, H. *Antimicrob. Agents Chemother.* **2009**, *53*, 997–1006.
9. (a) FDA approved Darunavir on June 23, 2006: FDA approved new HIV treatment for patients who do not respond to existing drugs. Please see: http://www.fda.gov/NewsEvents/Newsroom/PressAnnouncements/2006/ucm108676.htm (b) On October 21, 2008, FDA granted traditional approval to Prezista (darunavir), co-administered with ritonavir and with other antiretroviral agents, for the treatment of HIV-1 infection in treatment-experienced adult patients. In addition to the traditional approval, a new dosing regimen for treatment-naïve patients was approved.
10. Ghosh, A. K.; Chapsal, B. D.; Weber, I. T.; Mitsuya, H. *Acc. Chem. Res.* **2008**, *41*, 78–86.
11. Ghosh, A. K.; Ramu Sridhar, P.; Kumaragurubaran, N.; Koh, Y.; Weber, I. T.; Mitsuya, H. *ChemMedChem* **2006**, *1*, 939–950.
12. Mimoto, T.; Terashima, K.; Nojima, S.; Takaku, H.; Nakayama, M.; Shintani, M.; Yamaoka, T.; Hayashi, H. *Bioorg. Med. Chem.* **2004**, *12*, 281–293.
13. Yoshimura, K.; Kato, R.; Yusa, K.; Kavlick, M. F.; Maroun, V.; Nguyen, A.; Mimoto, T.; Ueno, T.; Shintani, M.; Falloon, J.; Masur, H.; Hayashi, H.; Erickson, J.; Mitsuya, H. *Proc. Natl. Acad. Sci. U.S.A.* **1999**, *96*, 8675–8680.
14. Ghosh, A. K.; Thompson, W. J.; Holloway, M. K.; McKee, S. P.; Duong, T. T.; Lee, H. Y.; Munson, P. M.; Smith, A. M.; Wai, J. M.; Darke, P. L.; Zugay, J.; Emini, E. A.; Schleif, W. A.; Huff, J. R.; Anderson, P. S. *J. Med. Chem.* **1993**, *36*, 2300–2310.
15. Ohmoto, K.; Okuma, M.; Yamamoto, T.; Kijima, H.; Sekioka, T.; Kitagawa, K.; Yamamoto, S.; Tanaka, K.; Kawabata, K.; Sakata, A., et al *Bioorg. Med. Chem. Lett.* **2001**, *9*, 1307–1323.
16. Ikunaka, M.; Matsumoto, J.; Nishimoto, Y. *Tetrahedron: Asymmetry* **2002**, *13*, 1201–1208.
17. Iwona Kudyba, I.; Raczko, J.; Jurczak, J. *J. Org. Chem.* **2004**, *69*, 2844–2850.
18. Ghosh, A. K.; Duong, T. T.; McKee, S. P. *Tetrahedron Lett.* **1992**, *33*, 2781–2784.
19. (a) Ghosh, A. K.; Leshchenko, S.; Noetzel, M. *J. Org. Chem.* **2004**, *69*, 7822–7829; (b) Ghosh, A. K.; Gemma, S.; Takayama, J.; Baldridge, A.; Leshchenko-Yashchuk, S.; Miller, H. B.; Wang, Y.-F.; Kovalevsky, A. Y.; Koh, Y.; Weber, I. T.; Mitsuya, H. *Org. Biomol. Chem.* **2008**, *6*, 3703–3713; (c) Ghosh, A. K.; Gemma, S.; Baldridge, A.; Wang, Y.-F.; Kovalevsky, A. Y.; Koh, Y.; Weber, I. T.; Mitsuya, H. *J. Med. Chem.* **2008**, *51*, 6021–6033.
20. Toth, M. V.; Marshall, G. R. A. *Int. J. Pep. Protein Res.* **1990**, *36*, 544–550.
21. Vega, S.; Kang, L.-W.; Velazquez-Campoy, A.; Kiso, Y.; Amzel, L. M.; Freire, E. *Proteins* **2004**, *55*, 594–602.
22. Kovalevski, A. Y.; Louis, J. M.; Aniana, A.; Ghosh, A. K.; Weber, I. T. *J. Mol. Biol.* **2008**, *384*, 178–192.

Biochemical and Biophysical Research Communications 408 (2011) 615–619

Contents lists available at ScienceDirect

Biochemical and Biophysical Research Communications

journal homepage: www.elsevier.com/locate/ybbrc

Dominant induction of vaccine antigen-specific cytotoxic T lymphocyte responses after simian immunodeficiency virus challenge

Yusuke Takahara [a,b], Saori Matsuoka [b], Tetsuya Kuwano [a], Tetsuo Tsukamoto [a], Hiroyuki Yamamoto [b], Hiroshi Ishii [a,b], Tadashi Nakasone [b], Akiko Takeda [b], Makoto Inoue [c], Akihiro Iida [c], Hiroto Hara [c], Tsugumine Shu [c], Mamoru Hasegawa [c], Hiromi Sakawaki [d], Mariko Horiike [d], Tomoyuki Miura [d], Tatsuhiko Igarashi [d], Taeko K. Naruse [e], Akinori Kimura [e], Tetsuro Matano [a,b,*]

[a] Division for AIDS Vaccine Development, The Institute of Medical Science, The University of Tokyo, 4-6-1 Shirokanedai, Minato-ku, Tokyo 108-8639, Japan
[b] AIDS Research Center, National Institute of Infectious Diseases, 1-23-1 Toyama, Shinjuku-ku, Tokyo 162-8640, Japan
[c] DNAVEC Corporation, 6 Ohkubo, Tsukuba, Ibaraki 300-2611, Japan
[d] Institute for Virus Research, Kyoto University, 53 Kawahara-cho, Shogoin, Sakyo-ku, Kyoto 606-8507, Japan
[e] Department of Molecular Pathogenesis, Medical Research Institute, Tokyo Medical and Dental University, 2-3-10 Kandasurugadai, Chiyoda-ku, Tokyo 101-0062, Japan

ARTICLE INFO

Article history:
Received 12 April 2011
Available online 21 April 2011

Keywords:
AIDS vaccine
HIV
SIV
CTL
Immunodominance

ABSTRACT

Cytotoxic T lymphocyte (CTL) responses are crucial for the control of human and simian immunodeficiency virus (HIV and SIV) replication. A promising AIDS vaccine strategy is to induce CTL memory resulting in more effective CTL responses post-viral exposure compared to those in natural HIV infections. We previously developed a CTL-inducing vaccine and showed SIV control in some vaccinated rhesus macaques. These vaccine-based SIV controllers elicited vaccine antigen-specific CTL responses dominantly in the acute phase post-challenge. Here, we examined CTL responses post-challenge in those vaccinated animals that failed to control SIV replication. Unvaccinated rhesus macaques possessing the major histocompatibility complex class I haplotype *90-088-Ij* dominantly elicited SIV non-Gag antigen-specific CTL responses after SIV challenge, while those induced with Gag-specific CTL memory by prophylactic vaccination failed to control SIV replication with dominant Gag-specific CTL responses in the acute phase, indicating dominant induction of vaccine antigen-specific CTL responses post-challenge even in non-controllers. Further analysis suggested that prophylactic vaccination results in dominant induction of vaccine antigen-specific CTL responses post-viral exposure but delays SIV non-vaccine antigen-specific CTL responses. These results imply a significant influence of prophylactic vaccination on CTL immunodominance post-viral exposure, providing insights into antigen design in development of a CTL-inducing AIDS vaccine.

© 2011 Elsevier Inc. All rights reserved.

1. Introduction

In human and simian immunodeficiency virus (HIV and SIV) infections, cytotoxic T lymphocyte (CTL) responses exert strong suppressive pressure on viral replication but fail to control viremia leading to AIDS progression [1–5]. A promising AIDS vaccine strategy is to induce CTL memory resulting in more effective CTL responses post-viral exposure compared to those in natural HIV infections. It is important to determine how prophylactic CTL memory induction affects CTL responses in the acute phase post-viral exposure.

We previously developed a prophylactic AIDS vaccine (referred to as DNA/SeV-Gag vaccine) consisting of DNA priming followed by boosting with a recombinant Sendai virus (SeV) vector expressing SIVmac239 Gag [6]. Evaluation of this vaccine's efficacy against a SIVmac239 challenge in Burmese rhesus macaques showed that some vaccinees contained SIV replication [7]. In particular, vaccination consistently resulted in SIV control in those animals possessing the major histocompatibility complex class I (MHC-I) haplotype *90-120-Ia* [8]; $Gag_{206-216}$ (IINEEAADWDL) and $Gag_{241-249}$ (SSVDEQIQW) epitope-specific CTL responses were shown to be responsible for this vaccine-based SIV control [9]. Furthermore, in a SIVmac239 challenge experiment of *90-120-Ia*-positive macaques that received a prophylactic DNA/SeV vaccine expressing the $Gag_{241-249}$ epitope fused with enhanced green fluorescent protein (EGFP), all the vaccinees controlled SIV replication [10]. This single epitope vaccination resulted in dominant $Gag_{241-249}$-specific CTL responses with delayed $Gag_{206-216}$-specific CTL induction after SIV challenge, whereas $Gag_{206-216}$-specific and

* Corresponding author at: AIDS Research Center, National Institute of Infectious Diseases, 1-23-1 Toyama, Shinjuku-ku, Tokyo 162-8640, Japan. Fax: +81 3 5285 1165.
E-mail address: tmatano@nih.go.jp (T. Matano).

0006-291X/$ - see front matter © 2011 Elsevier Inc. All rights reserved.
doi:10.1016/j.bbrc.2011.04.071

$Gag_{241-249}$-specific CTL responses were detected equivalently in unvaccinated *90-120-Ia*-positive animals.

These previous results in vaccine-based SIV controllers indicate dominant induction of vaccine antigen-specific CTL responses post-challenge, implying that prophylactic vaccination inducing vaccine antigen-specific CTL memory may delay CTL responses specific for viral antigens other than vaccine antigens (referred to as non-vaccine antigens) post-viral exposure. In these SIV controllers, the reduction of viral loads could be involved in delay of SIV non-vaccine antigen-specific CTL responses. Then, in the present study, we examined the influence of prophylactic vaccination on immunodominance post-challenge in those vaccinees that failed to control SIV replication. Our results showed dominant induction of vaccine antigen-specific CTL responses post-challenge even in these SIV non-controllers.

2. Materials and methods

2.1. Animal experiments

The first set of experiment used samples in our previous experiments of six Burmese rhesus macaques (Macaca mulatta) possessing the MHC-I haplotype *90-088-Ij* (macaques R02-004, R02-001, and R03-015, previously reported [7,11]; R04-014, R06-022, and R04-011, unpublished). Three of them, R02-001, R04-011, and R03-015, received a prophylactic DNA/SeV-Gag vaccine [7]. The DNA used for the vaccination, CMV-SHIVdEN, was constructed from *env*-deleted and *nef*-deleted simian–human immunodeficiency virus $SHIV_{MD14YE}$ [12] molecular clone DNA (SIVGP1) and has the genes encoding SIVmac239 Gag, Pol, Vif, and Vpx, SIVmac239-HIV chimeric Vpr, and HIV Tat and Rev. At the DNA vaccination, animals received 5 mg of CMV-SHIVdEN DNA intramuscularly. Six weeks after the DNA prime, animals received a single boost intranasally with 6×10^9 cell infectious units (CIUs) of F-deleted replication-defective SeV-Gag [13,14]. All six *90-088-Ij*-positive animals including three unvaccinated and three vaccinated were challenged intravenously with 1000 50% tissue culture infective doses (TCID50) of SIVmac239 [15] approximately 3 months after the boost. At week 1 after SIV challenge, macaque R03-015 was inoculated with nonspecific immunoglobulin G as previously described [11].

In the second set of experiment, unvaccinated (R06-001) and vaccinated (R05-028) rhesus macaques possessing the MHC-I haplotype *90-120-Ib* were challenged intravenously with 1000 TCID50 of SIVmac239. The latter R05-028 were immunized intranasally with F-deleted SeV-Gag approximately 3 months before the challenge.

In the third, three rhesus macaques received FMSIV plus mCAT1-expressing DNA vaccination three times with intervals of 4 weeks. The FMSIV DNA was constructed by replacing *nef*-deleted $SHIV_{MD14YE}$ with Friend murine leukemia virus (FMLV) *env*, carrying the same SIVmac239-derived antigen-coding regions with SIVGP1, as described before [16]. Vaccination of macaques with FMSIV and a DNA expressing the FMLV receptor (mCAT1) [17] three times with intervals of a week was previously shown to induce mCAT1-dependent confined FMSIV replication resulting in efficient CTL induction while vaccination three times with intervals of 4 weeks in the present study resulted in marginal levels of responses (data not shown). These three DNA-vaccinated animals were challenged intravenously with 1000 TCID50 of SIVmac239 approximately 2 months after the last vaccination.

Some animal experiments were conducted in the Tsukuba Primate Research Center, National Institute of Biomedical Innovation, with the help of the Corporation for Production and Research of Laboratory Primates, in accordance with the guidelines for animal experiments at the National Institute of Infectious Diseases, and others were in Institute for Virus Research, Kyoto University in accordance with the institutional regulations.

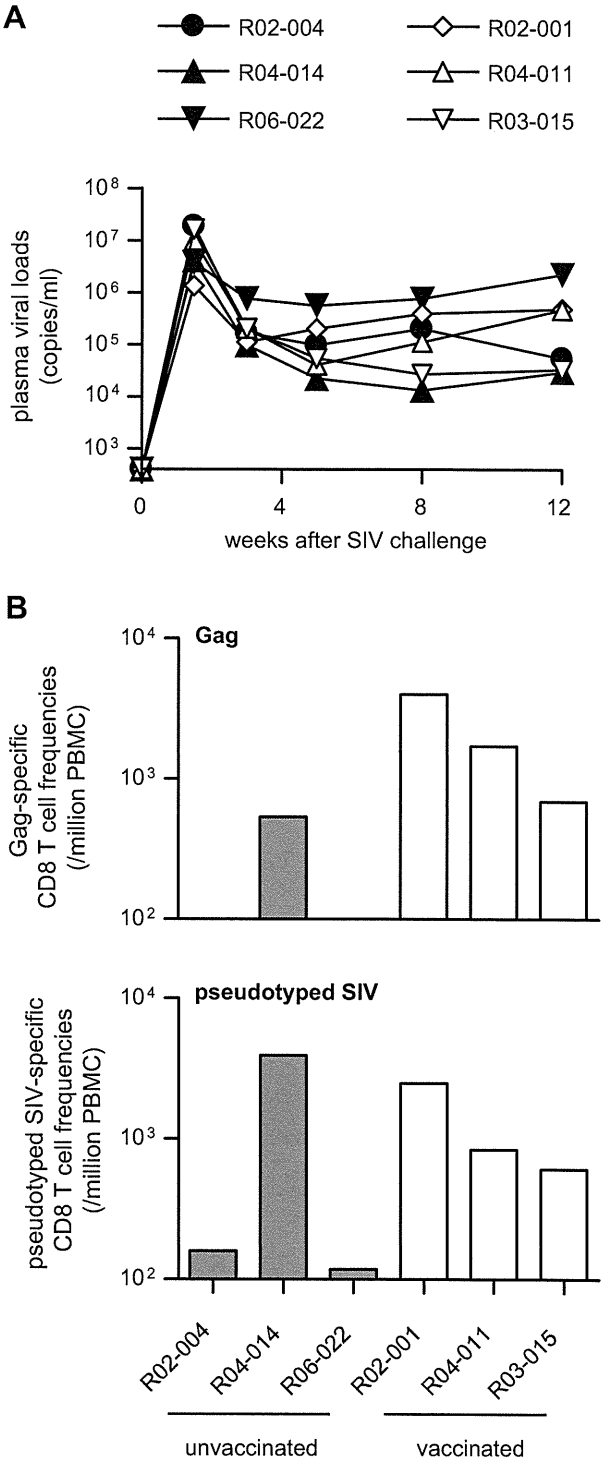

Fig. 1. CTL responses after SIVmac239 challenge in *90-088-Ij*-positive macaques. (A) Plasma viral loads after SIV challenge in unvaccinated (R02-004, R04-014, and R06-022) and DNA/SeV-Gag vaccinated animals (R02-001, R04-011, and R03-015). The viral loads (SIV gag RNA copies/ml) were determined as described previously [7]. (B) Vaccine antigen Gag-specific (upper panel) and pseudotyped SIV-specific $CD8^+$ T cell frequencies (lower panel) at week 2 after SIV challenge.

2.2. Analysis of virus-specific CTL responses

We measured virus-specific $CD8^+$ T-cell levels by flow cytometric analysis of gamma interferon (IFN-γ) induction after specific

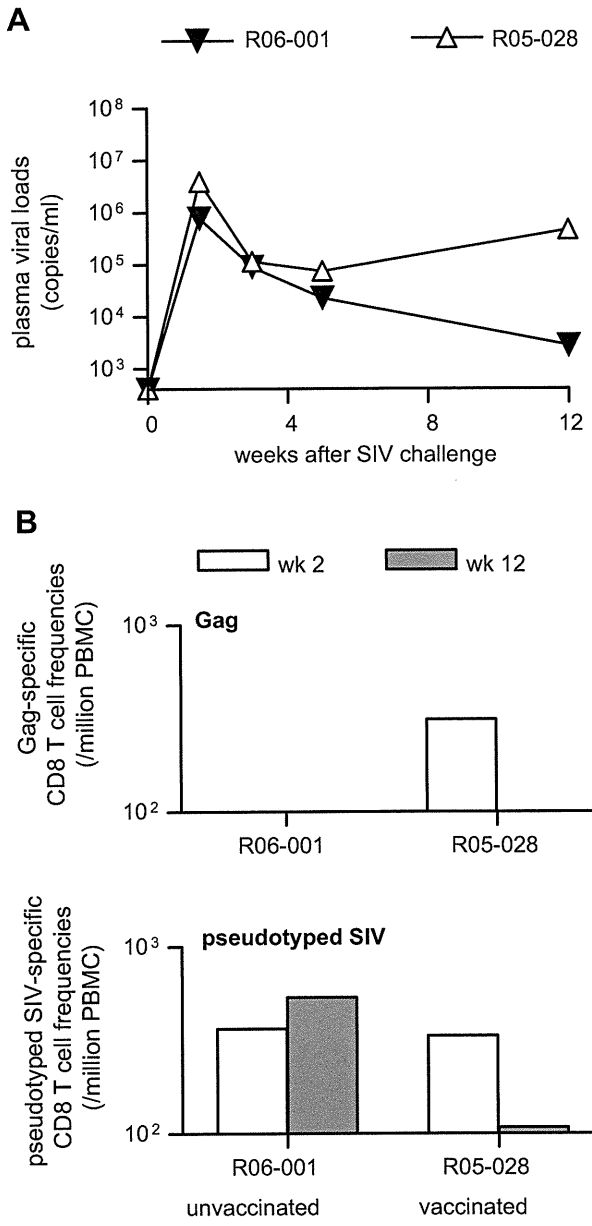

Fig. 2. CTL responses after SIVmac239 challenge in *90–120-Ib*-positive macaques. (A) Plasma viral loads after SIV challenge in unvaccinated R06-001 and SeV-Gag-vaccinated macaque R05-028. (B) Vaccine antigen Gag-specific (upper panel) and pseudotyped SIV-specific $CD8^+$ T cell frequencies (lower panel) at weeks 2 (white bars) and 12 (black bars) after SIV challenge.

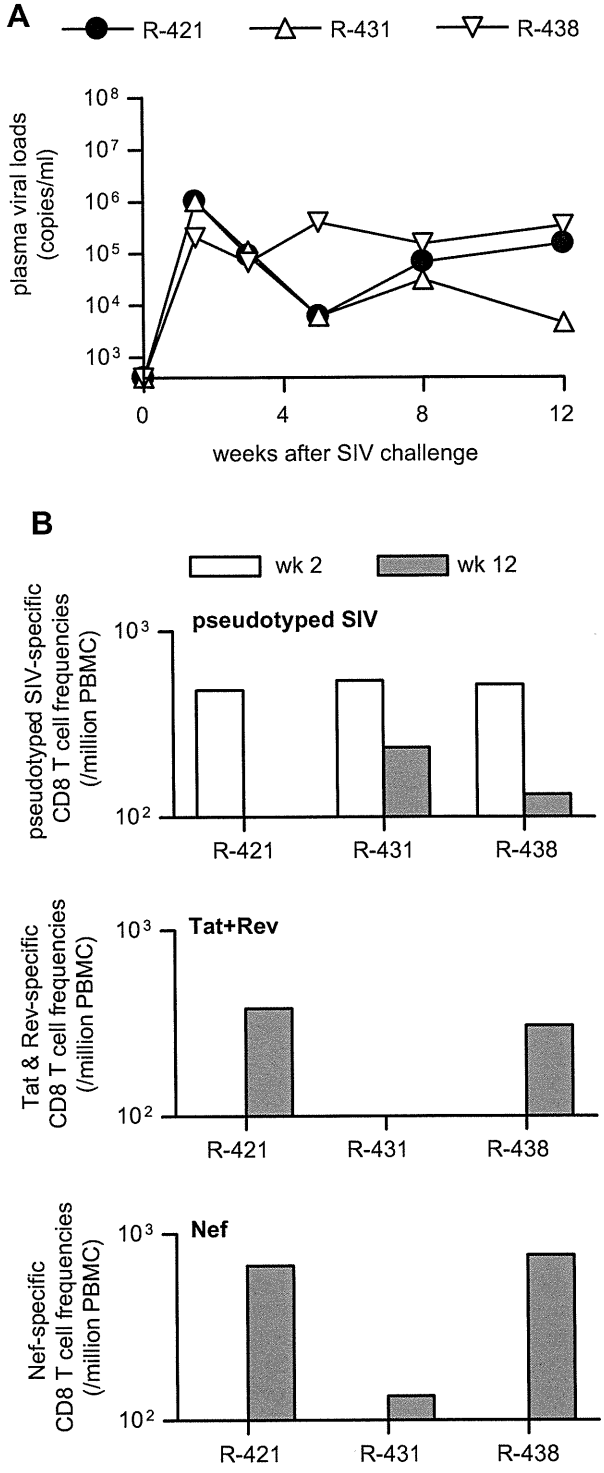

Fig. 3. CTL responses after SIVmac239 challenge in DNA-vaccinated macaques. The DNA used for the vaccination has the SIVmac239-derived region encoding Gag, Pol, Vif, and Vpx and is expected to induce pseudotyped SIV-specific CTL responses. (A) Plasma viral loads after SIV challenge in DNA vaccinated macaques R-421, R-431, and R-438. (B) Vaccine antigen (pseudotyped SIV)-specific (top panel), Tat-plus-Rev-specific (middle panel), and Nef-specific $CD8^+$ T cell frequencies (bottom panel) at weeks 2 (white bars) and 12 (black bars) after SIV challenge. In macaque R-438, CTL responses at week 5 instead of week 12 are shown.

stimulation as described previously [18,19]. Peripheral blood mononuclear cells (PBMCs) were cocultured with autologous herpesvirus papio-immortalized B-lymphoblastoid cell lines (B-LCLs) infected with a vaccinia virus vector expressing SIVmac239 Gag for Gag-specific stimulation or a vesicular stomatitis virus G protein (VSV-G)-pseudotyped SIV for pseudotyped SIV-specific stimulation. The pseudotyped SIV was obtained by cotransfection of COS-1 cells with a VSV-G-expression plasmid and SIVGP1 DNA. Alternatively, PBMCs were cocultured with B-LCLs pulsed with peptide pools using panels of overlapping peptides spanning the entire SIVmac239 Tat, Rev, and Nef amino acid sequences. Intracellular IFN-γ staining was performed with a CytofixCytoperm kit (Becton Dickinson, Tokyo, Japan) and fluorescein isothiocyanate-conjugated anti-human CD4, peridinin chlorophyll protein-conjugated anti-human CD8, allophycocyanin-conjugated anti-human CD3, and phycoerythrin-conjugated anti-human IFN-γ monoclonal antibodies (Becton Dickinson). Specific $CD8^+$ T-cell levels were calculated by subtracting nonspecific IFN-γ^+ $CD8^+$ T-cell frequencies from those after Gag-specific, pseudotyped

	vaccine antigen					non-vaccine antigen										
	Gag				Vif	Vpr	Tat					Rev		Nef		
	165	333	375	376	143	73	23	115	120	122	125	45	50	63	100	124
wk 5																
R- 421					++											
R- 431					+											
R- 438	++		+							++						
wk 12																
R- 421		++			++				+		+	+	+			++
R- 431					+		+			++						
R- 438	++			++		+		++						++	++	

Fig. 4. Viral mutations in DNA-vaccinated macaques. Plasma viral genome sequencing was performed as described previously [18] to determine mutations resulting in amino acid substitutions in SIV Gag, Pol, Vif, Vpx, Vpr, Tat, Rev, and Nef antigens (except for Env) at weeks 5 and 12 in DNA-vaccinated macaques. The amino acid positions showing mutant sequences dominantly (++) or equivalently with wild type (+) are shown. While we found a mutation leading to a lysine-to-arginine alteration at the 40th amino acid in Rev in all animals, this mutation is not shown because the wild-type sequence at this position in the SIVmac239 molecular clone is considered to be a suboptimal nucleotide that frequently reverts to an alternative sequence in vivo [18,23].

SIV-specific, or peptide-specific stimulation. Specific $CD8^+$ T-cell levels lower than 100 per million PBMCs were considered negative.

3. Results and discussion

In our previous SIVmac239 challenge experiments, the prophylactic DNA/SeV-Gag vaccination did not result in viral control in rhesus macaques possessing the MHC-I haplotype *90-088-Ij*. These vaccinated animals showed similar levels of plasma viral loads as those in unvaccinated *90-088-Ij*-positive animals after SIV challenge (Fig. 1A). Analysis of virus-specific $CD8^+$ T-cell responses using PBMCs at week 2 after challenge showed equivalent Gag-specific and pseudotyped SIV-specific (Gag-, Pol-, Vif-, and Vpx-specific) CTL responses in all three vaccinees (Fig. 1B). Pseudotyped SIV-specific CTL responses were also detected in all three unvaccinated animals, but Gag-specific CTL responses were undetectable in two out of the three; even the Gag-specific CTL responses detected in macaque R04-014 were much lower than pseudotyped SIV-specific CTL responses, indicating dominant induction of CTL responses specific for SIV antigens other than Gag (Fig. 1B). Thus, in the acute phase of SIV infection, SIV non-Gag antigen-specific CTL responses were dominantly induced in unvaccinated *90-088-Ij*-positive macaques, whereas vaccine antigen (Gag)-specific CTL responses were dominant in *90-088-Ij*-positive vaccinees.

We then analyzed another vaccinees that failed to control a SIVmac239 challenge; these macaques were vaccinated with SeV-Gag alone or DNA alone. First, we compared post-challenge CTL responses in unvaccinated and SeV-Gag-vaccinated macaques possessing the MHC-I haplotype *90-120-Ib*. Both macaques failed to control SIV replication after challenge (Fig. 2A). In the unvaccinated animal R06-001, Gag-specific CTL responses were undetectable but pseudotyped SIV-specific CTL responses were induced efficiently at weeks 2 and 12 (Fig. 2B). In contrast, Gag-specific CTL responses were induced efficiently at week 2 in the SeV-Gag-vaccinated animal R05-028 (Fig. 2B). At week 12, Gag-specific CTL responses became undetectable while pseudotyped SIV-specific CTL responses were still detectable in this animal. These results indicate that, in the acute phase after SIVmac239 challenge, the unvaccinated *90-120-Ib*-positive macaque dominantly elicited SIV non-Gag antigen-specific CTL responses whereas the SeV-Gag-vaccinated *90-120-Ib*-positive macaque dominantly induced vaccine antigen (Gag)-specific CTL responses.

Next, we analyzed post-challenge CTL responses in three DNA-vaccinated macaques. These animals failed to control SIVmac239 replication after challenge (Fig. 3A). The DNA used for the vaccination and the pseudotyped SIV genome both have the same SIVmac239-derived region encoding Gag, Pol, Vif, and Vpx, thus expected to induce pseudotyped SIV-specific CTL responses. Pseudotyped SIV-specific CTL responses, namely vaccine antigen-specific CTL responses, were induced efficiently at week 2 but diminished after that in all three animals (Fig. 3B). In contrast, Tat/Rev- and Nef-specific CTL responses were undetectable at week 2 but induced later (Fig. 3B). Again, vaccine antigen-specific CTL responses were dominantly induced in the acute phase after SIV challenge and non-vaccine antigen-specific CTL responses were elicited later.

All three animals showed viral genome mutations leading to amino acid substitutions in Gag or Vif at week 5 (Fig. 4). Further analysis indicated that viral mutations in vaccine antigen-coding regions appeared earlier than those in other regions. These results may reflect selective pressure on SIV by vaccine antigen-specific CTL responses dominantly induced in the acute phase, although it remains undetermined whether these mutations are CTL escape ones. Disappearance of vaccine antigen-specific CTL responses at week 12 may be explained by rapid selection of CTL escape mutations in vaccine antigen-coding regions. However, analysis using peptides found Gag-specific CTL responses in macaques R-421 and R-431 that had no gag mutations at week 5 (data not shown), suggesting involvement of immunodominance [20] in the disappearance of vaccine antigen-specific CTL responses at week 12.

In summary, the present study indicates that vaccine antigen-specific CTL responses are induced dominantly in the acute phase after viral exposure, with delayed induction of CTL responses specific for SIV non-vaccine antigens (SIV antigens other than vaccine antigens). While this delay previously-observed in vaccine-based SIV controllers [10] can be explained not only by immunodominance but also by reduction in viral loads, the delay in vaccinated non-controllers in the present study might reflect the immunodominance in CTL responses. Thus, in development of a prophylactic, CTL-inducing AIDS vaccine, it is important to select vaccine antigens leading to effective CTL responses post-viral

exposure [21,22]. These results imply a significant influence of prophylactic vaccination on the immunodominance pattern of CTL responses post-viral exposure, providing insights into antigen design in development of a CTL-inducing AIDS vaccine.

Acknowledgments

This work was supported by Grants-in-aid from the Ministry of Education, Culture, Sports, Science, and Technology, Grants-in-aid from the Ministry of Health, Labor, and Welfare, and a Grant from Takeda Science Foundation in Japan.

References

[1] R.A. Koup, J.T. Safrit, Y. Cao, C.A. Andrews, G. McLeod, W. Borkowsky, C. Farthing, D.D. Ho, Temporal association of cellular immune responses with the initial control of viremia in primary human immunodeficiency virus type 1 syndrome, J. Virol. 68 (1994) 4650–4655.

[2] P. Borrow, H. Lewicki, B.H. Hahn, G.M. Shaw, M.B. Oldstone, Virus-specific CD8$^+$ cytotoxic T-lymphocyte activity associated with control of viremia in primary human immunodeficiency virus type 1 infection, J. Virol. 68 (1994) 6103–6110.

[3] T. Matano, R. Shibata, C. Siemon, M. Connors, H.C. Lane, M.A. Martin, Administration of an anti-CD8 monoclonal antibody interferes with the clearance of chimeric simian/human immunodeficiency virus during primary infections of rhesus macaques, J. Virol. 72 (1998) 164–169.

[4] X. Jin, D.E. Bauer, S.E. Tuttleton, S. Lewin, A. Gettie, J. Blanchard, C.E. Irwin, J.T. Safrit, J. Mittler, L. Weinberger, L.G. Kostrikis, L. Zhang, A.S. Perelson, D.D. Ho, Dramatic rise in plasma viremia after CD8(+) T cell depletion in simian immunodeficiency virus-infected macaques, J. Exp. Med. 189 (1999) 991–998.

[5] P.J. Goulder, D.I. Watkins, HIV and SIV CTL escape: implications for vaccine design, Nat. Rev. Immunol. 4 (2004) 630–640.

[6] T. Matano, M. Kano, H. Nakamura, A. Takeda, Y. Nagai, Rapid appearance of secondary immune responses and protection from acute CD4 depletion after a highly pathogenic immunodeficiency virus challenge in macaques vaccinated with a DNA prime/Sendai virus vector boost regimen, J. Virol. 75 (2001) 11891–11896.

[7] T. Matano, M. Kobayashi, H. Igarashi, A. Takeda, H. Nakamura, M. Kano, C. Sugimoto, K. Mori, A. Iida, T. Hirata, M. Hasegawa, T. Yuasa, M. Miyazawa, Y. Takahashi, M. Yasunami, A. Kimura, D.H. O'Connor, D.I. Watkins, Y. Nagai, Cytotoxic T lymphocyte-based control of simian immunodeficiency virus replication in a preclinical AIDS vaccine trial, J. Exp. Med. 199 (2004) 1709–1718.

[8] Y. Takahashi-Tanaka, M. Yasunami, T. Naruse, K. Hinohara, T. Matano, K. Mori, M. Miysazawa, M. Honda, Y. Yasutomi, Y. Nagai, A. Kimura, Reference strand-mediated conformation analysis (RSCA)-based typing of multiple alleles in the rhesus macaque MHC class I Mamu-A and Mamu-B loci, Electrophoresis 28 (2007) 918–924.

[9] M. Kawada, T. Tsukamoto, H. Yamamoto, N. Iwamoto, K. Kurihara, A. Takeda, C. Moriya, H. Takeuchi, H. Akari, T. Matano, Gag-specific cytotoxic T lymphocyte-based control of primary simian immunodeficiency virus replication in a vaccine trial, J. Virol. 82 (2008) 10199–10206.

[10] T. Tsukamoto, A. Takeda, T. Yamamoto, H. Yamamoto, M. Kawada, T. Matano, Impact of cytotoxic-T-lymphocyte memory induction without virus-specific CD4+ T-Cell help on control of a simian immunodeficiency virus challenge in rhesus macaques, J. Virol. 83 (2009) 9339–9346.

[11] H. Yamamoto, M. Kawada, A. Takeda, H. Igarashi, T. Matano, Post-infection immunodeficiency virus control by neutralizing antibodies, PLoS ONE 2 (2007) e540.

[12] R. Shibata, F. Maldarelli, C. Siemon, T. Matano, M. Parta, G. Miller, T. Fredrickson, M.A. Martin, Infection and pathogenicity of chimeric simian-human immunodeficiency viruses in macaques: determinants of high virus loads and CD4 cell killing, J. Infect. Dis. 176 (1997) 362–373.

[13] H.O. Li, Y.F. Zhu, M. Asakawa, H. Kuma, T. Hirata, Y. Ueda, Y.S. Lee, M. Fukumura, A. Iida, A. Kato, Y. Nagai, M. Hasegawa, A cytoplasmic RNA vector derived from nontransmissible Sendai virus with efficient gene transfer and expression, J. Virol. 74 (2000) 6564–6569.

[14] A. Takeda, H. Igarashi, H. Nakamura, M. Kano, A. Iida, T. Hirata, M. Hasegawa, Y. Nagai, T. Matano, Protective efficacy of an AIDS vaccine, a single DNA priming followed by a single booster with a recombinant replication-defective Sendai virus vector, in a macaque AIDS model, J. Virol. 77 (2003) 9710–9715.

[15] H.W. Kestler 3rd, D.J. Ringler, K. Mori, D.L. Panicali, P.K. Sehgal, M.D. Daniel, R.C. Desrosiers, Importance of the nef gene for maintenance of high virus loads and for development of AIDS, Cell 65 (1991) 651–662.

[16] T. Matano, M. Kano, T. Odawara, H. Nakamura, A. Takeda, K. Mori, T. Sato, Y. Nagai, Induction of protective immunity against pathogenic simian immunodeficiency virus by a foreign receptor-dependent replication of an engineered avirulent virus, Vaccine 18 (2000) 3310–3318.

[17] L.M. Albritton, L. Tweng, D. Scadden, J.M. Cunningham, A putative murine retrovirus receptor gene encodes a multiple membrane-spanning protein and confers susceptibility to virus infection, Cell 57 (1989) 659–666.

[18] M. Kawada, T. Tsukamoto, H. Yamamoto, A. Takeda, H. Igarashi, D.I. Watkins, T. Matano, Long-term control of simian immunodeficiency virus replication with central memory CD4$^+$ T-cell preservation after nonsterile protection by a cytotoxic T-lymphocyte-based vaccine, J. Virol. 81 (2007) 5202–5211.

[19] N. Iwamoto, T. Tsukamoto, M. Kawada, A. Takeda, H. Yamamoto, H. Takeuchi, T. Matano, Broadening of CD8$^+$ cell responses in vaccine-based simian immunodeficiency virus controllers, AIDS 24 (2010) 2777–2787.

[20] S. Tenzer, E. Wee, A. Burgevin, G. Stewart-Jones, L. Friis, K. Lamberth, C.H. Chang, M. Harndahl, M. Weimershaus, J. Gerstoft, N. Akkad, P. Klenerman, L. Fugger, E.Y. Jones, A.J. McMichael, S. Buus, H. Schild, P. van Endert, A.K. Iversen, Antigen processing influences HIV-specific cytotoxic T lymphocyte immunodominance, Nat. Immunol. 10 (2009) 636–646.

[21] P.J.R. Goulder, D.I. Watkins, Impact of MHC class I diversity on immune control of immunodeficiency virus replication, Nat. Rev. Immunol. 8 (2008) 619–630.

[22] H. Streeck, J.S. Jolin, Y. Qi, B. Yassine-Diab, R.C. Johnson, D.S. Kwon, M.M. Addo, C. Brumme, J.P. Routy, S. Little, H.K. Jessen, A.D. Kelleher, F.M. Hecht, R.P. Sekaly, E.S. Rosenberg, B.D. Walker, M. Carrington, M. Altfeld, Human immunodeficiency virus type 1-specific CD8$^+$ T-cell responses during primary infection are major determinants of the viral set point and loss of CD4+ T cells, J. Virol. 83 (2009) 7641–7648.

[23] L. Alexander, L. Denekamp, S. Czajak, R.C. Desrosiers, Suboptimal nucleotides in the infectious, pathogenic simian immunodeficiency virus clone SIVmac239, J. Virol. 75 (2001) 4019–4022.

JVI
Journals.ASM.org

Impact of Vaccination on Cytotoxic T Lymphocyte Immunodominance and Cooperation against Simian Immunodeficiency Virus Replication in Rhesus Macaques

Hiroshi Ishii,[a,b] Miki Kawada,[b] Tetsuo Tsukamoto,[b] Hiroyuki Yamamoto,[a] Saori Matsuoka,[a] Teiichiro Shiino,[a] Akiko Takeda,[a] Makoto Inoue,[c] Akihiro Iida,[c] Hiroto Hara,[c] Tsugumine Shu,[c] Mamoru Hasegawa,[c] Taeko K. Naruse,[d] Akinori Kimura,[d] Masafumi Takiguchi,[e] and Tetsuro Matano[a,b]

AIDS Research Center, National Institute of Infectious Diseases, Tokyo, Japan[a]; Institute of Medical Science, University of Tokyo, Tokyo, Japan[b]; DNAVEC Corporation, Tsukuba, Japan[c]; Department of Molecular Pathogenesis, Medical Research Institute, Tokyo Medical and Dental University, Tokyo, Japan[d]; and Center for AIDS Research, Kumamoto University, Kumamoto, Japan[e]

Cytotoxic T lymphocyte (CTL) responses play a central role in viral suppression in human immunodeficiency virus (HIV) infections. Prophylactic vaccination resulting in effective CTL responses after viral exposure would contribute to HIV control. It is important to know how CTL memory induction by vaccination affects postexposure CTL responses. We previously showed vaccine-based control of a simian immunodeficiency virus (SIV) challenge in a group of Burmese rhesus macaques sharing a major histocompatibility complex class I haplotype. $Gag_{206-216}$ and $Gag_{241-249}$ epitope-specific CTL responses were responsible for this control. In the present study, we show the impact of individual epitope-specific CTL induction by prophylactic vaccination on postexposure CTL responses. In the acute phase after SIV challenge, dominant $Gag_{206-216}$-specific CTL responses with delayed, naive-derived $Gag_{241-249}$-specific CTL induction were observed in $Gag_{206-216}$ epitope-vaccinated animals with prophylactic induction of single $Gag_{206-216}$ epitope-specific CTL memory, and vice versa in $Gag_{241-249}$ epitope-vaccinated animals with single $Gag_{241-249}$ epitope-specific CTL induction. Animals with $Gag_{206-216}$-specific CTL induction by vaccination selected for a $Gag_{206-216}$-specific CTL escape mutation by week 5 and showed significantly less decline of plasma viral loads from week 3 to week 5 than in $Gag_{241-249}$ epitope-vaccinated animals without escape mutations. Our results present evidence indicating significant influence of prophylactic vaccination on postexposure CTL immunodominance and cooperation of vaccine antigen-specific and non-vaccine antigen-specific CTL responses, which affects virus control. These findings provide great insights into antigen design for CTL-inducing AIDS vaccines.

Human immunodeficiency virus (HIV) infection induces chronic, persistent viral replication leading to AIDS onset in humans. Virus-specific cytotoxic T lymphocyte (CTL) responses play a central role in the resolution of acute peak viremia (3, 4, 13, 22, 28) but mostly fail to contain viral replication in the natural course of HIV infection. Vaccination resulting in more effective CTL responses after viral exposure than in natural HIV infections would contribute to HIV control (30, 33). CTL memory induction by prophylactic vaccination may lead to efficient secondary CTL responses, but naive-derived primary CTL responses specific for viral nonvaccine antigens can also be induced after viral exposure. It is important to know how CTL memory induction by vaccination affects these postexposure CTL responses.

Cumulative studies on HIV-infected individuals have shown association of HLA genotypes with rapid or delayed AIDS progression (5, 14, 31, 34). For instance, most of the HIV-infected individuals possessing *HLA-B*57* have been indicated to show a better prognosis with lower viral loads, implicating HLA-B*57-restricted epitope-specific CTL responses in this viral control (1, 8, 23, 24). Indian rhesus macaques possessing certain major histocompatibility complex class I (MHC-I) alleles, such as *Mamu-A*01*, *Mamu-B*08*, and *Mamu-B*17*, tend to show simian immunodeficiency virus (SIV) control (19, 25, 36). This implies possible HIV control by induction of particular effective CTL responses (2, 7, 12, 16, 27).

Recent trials of prophylactic T-cell-based vaccines in macaque AIDS models have indicated the possibility of reduction in post-challenge viral loads (6, 15, 17, 21, 35). We previously developed a prophylactic AIDS vaccine consisting of a DNA prime and a boost with a Sendai virus (SeV) vector expressing SIVmac239 Gag (SeV-Gag) (20). Our trial showed vaccine-based control of an SIVmac239 challenge in a group of Burmese rhesus macaques sharing the MHC-I haplotype *90-120-Ia* (21). Animals possessing *90-120-Ia* dominantly elicited Mamu-A1*043:01 (GenBank accession number AB444869)-restricted $Gag_{206-216}$ (IINEEAADWDL) epitope-specific and Mamu-A1*065:01 (AB444921)-restricted $Gag_{241-249}$ (SSVDEQIQW) epitope-specific CTL responses after SIV challenge and selected for viral *gag* mutations, GagL216S (leading to a leucine [L]-to-serine [S] substitution at amino acid [aa] 216 in Gag) and GagD244E (aspartic acid [D]-to-glutamic acid [E] at aa 244), resulting in escape from CTL recognition with viral fitness costs in the chronic phase (9, 26). Vaccinees possessing *90-120-Ia* failed to control a challenge with a mutant SIV carrying these two CTL escape mutations, indicating that $Gag_{206-216}$-specific and $Gag_{241-249}$-specific CTL responses play a crucial role in the vaccine-based control of wild-type SIVmac239 replication

Received 5 September 2011 Accepted 31 October 2011
Published ahead of print 9 November 2011
Address correspondence to Tetsuro Matano, tmatano@nih.go.jp.
Copyright © 2012, American Society for Microbiology. All Rights Reserved.
doi:10.1128/JVI.06226-11

TABLE 1 Animals analyzed in this study

Group	No. of animals	Vaccination[a]	SIV-specific CTL response postboost
I	6	None	None
II	5	Gag (pCMV-SHIVdEN DNA prime, SeV-Gag boost)	Gag-specific CTL
III	6	$Gag_{241-249}$-specific (p$Gag_{236-250}$-EGFP-N1 DNA prime, SeV-$Gag_{236-250}$-EGFP boost)	$Gag_{241-249}$-specific CTL
IV	5	$Gag_{206-216}$-specific (p$Gag_{202-216}$-EGFP-N1 DNA prime, SeV-$Gag_{202-216}$-EGFP boost)	$Gag_{206-216}$-specific CTL

[a] All animals were challenged with SIVmac239.

(10). Furthermore, in an SIVmac239 challenge experiment with *90-120-Ia*-positive rhesus macaques that received a prophylactic vaccine expressing the $Gag_{241-249}$ epitope fused with enhanced green fluorescent protein (EGFP), this single-epitope vaccination resulted in control of SIVmac239 replication with dominant induction of $Gag_{241-249}$-specific CTL responses in the acute phase postchallenge (32).

Thus, it is hypothesized that induction of single $Gag_{206-216}$ or $Gag_{241-249}$ epitope-specific CTL responses by vaccination may result in different patterns of CTL immunodominance and viral replication after SIV challenge. In the present study, we analyzed the impact of prophylactic vaccination inducing single $Gag_{206-216}$ epitope-specific CTL responses on SIV control in *90-120-Ia*-positive macaques and compared the results with those of vaccination inducing single $Gag_{241-249}$ epitope-specific CTL responses. This analysis revealed differences in CTL responses and patterns of viral control after SIV challenge between these vaccinated groups, indicating significant effects of prophylactic vaccination on postexposure CTL immunodominance and cooperation of vaccine antigen-specific and non-vaccine antigen-specific CTL responses.

MATERIALS AND METHODS

Animal experiments. Animal experiments were conducted through the Cooperative Research Program at Tsukuba Primate Research Center, National Institute of Biomedical Innovation, with the help of the Corporation for Production and Research of Laboratory Primates. Blood collection, vaccination, and virus challenge were performed under ketamine anesthesia. All animals were maintained in accordance with the Guideline for Laboratory Animals of the National Institute of Infectious Diseases.

Five Burmese rhesus macaques (*Macaca mulatta*) possessing the MHC-I haplotype *90-120-Ia* (26) (group IV) received a DNA-prime/SeV-boost vaccine eliciting $Gag_{206-216}$-specific CTL responses followed by an SIVmac239 challenge and were compared with three groups (I, II, and III) of *90-120-Ia*-positive animals reported previously (10, 32) (Table 1). Group I animals ($n = 6$) received no vaccination, while group II animals ($n = 5$) received a DNA-prime/SeV-boost vaccine eliciting Gag-specific CTL responses. The DNA, CMV-SHIVdEN, used for the vaccination was constructed from a simian/human immunodeficiency virus ($SHIV_{MD14YE}$) molecular clone DNA with *env* and *nef* deleted (29) and has the genes encoding SIVmac239 Gag, Pol, Vif, and Vpx; SIVmac239–HIV-1 chimeric Vpr; and HIV-1 Tat and Rev (21). In group II animals, CTL responses were undetectable after DNA prime but Gag-specific CTL responses became detectable after SeV-Gag boost. Group III animals ($n = 6$) received a DNA-prime/SeV-boost vaccine eliciting $Gag_{241-249}$-specific CTL responses. A p$Gag_{236-250}$-EGFP-N1 DNA and an SeV-$Gag_{236-250}$-EGFP vector, both expressing an SIVmac239 $Gag_{236-250}$ (IAGTTSSVDEQ IQWM)-EGFP fusion protein, were used for the group III vaccination. After the SeV-$Gag_{236-250}$-EGFP boost, group III animals induced $Gag_{241-249}$-specific CTL responses; the animals showed no $Gag_{236-250}$-specific $CD4^+$ T-cell responses but elicited SeV/EGFP-specific $CD4^+$ T-cell responses (32). For the group IV vaccination, A p$Gag_{202-216}$-EGFP-N1 DNA and an SeV-$Gag_{202-216}$-EGFP vector, both expressing an SIVmac239 $Gag_{202-216}$ (IIRDIINEEAADWDL)-EGFP fusion protein, were used (Fig. 1). Approximately 3 months after the boost, all animals were challenged intravenously with 1,000 50% tissue culture infective doses of SIVmac239 (11). In our previous study (32), the unvaccinated and the control-vaccinated

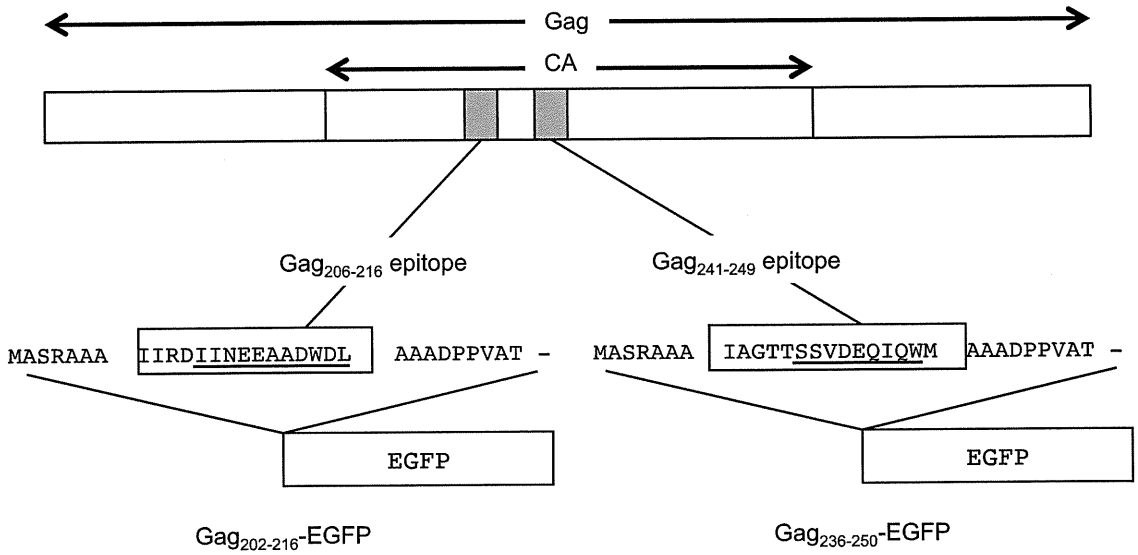

FIG 1 Schema of the cDNA constructs encoding $Gag_{202-216}$-EGFP and $Gag_{236-250}$-EGFP fusion proteins. A DNA fragment that encodes a 31-mer peptide (boxes) including the $Gag_{202-216}$ or $Gag_{236-250}$ sequence (underlining) was introduced into the 5′ end of the EGFP cDNA.

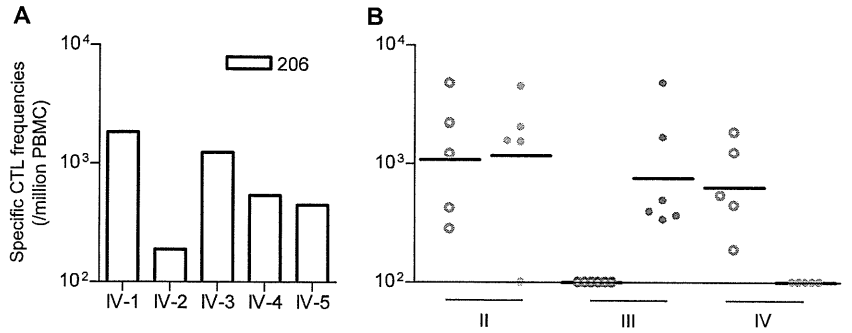

FIG 2 $Gag_{206-216}$-specific and $Gag_{241-249}$-specific CTL responses after prophylactic vaccination. (A) $Gag_{206-216}$-specific $CD8^+$ T-cell frequencies 1 week after SeV-$Gag_{202-216}$–EGFP boost in group IV macaques (open boxes). (B) $Gag_{206-216}$-specific (open circles) and $Gag_{241-249}$-specific (closed circles) $CD8^+$ T-cell frequencies 1 week after boost in group II (green), III (blue), and IV (red) macaques. The bars indicate the geometric mean of each group. No animal showed detectable Gag-specific CTL responses before the boost.

animals receiving a DNA and an SeV expressing EGFP showed no significant differences in viral loads after SIV challenge.

Analysis of antigen-specific CTL responses. We measured virus-specific $CD8^+$ T-cell levels by flow cytometric analysis of gamma interferon (IFN-γ) induction after specific stimulation, as described previously (21). Peripheral blood mononuclear cells (PBMCs) were cocultured with autologous herpesvirus papioimmortalized B-lymphoblastoid cell lines pulsed with 1 μM SIVmac239 $Gag_{206-216}$ (IINEEAADWDL), $Gag_{241-249}$ (SSVDEQIQW), or $Gag_{367-381}$ (ALKEALAPVPIPFAA) peptide for $Gag_{206-216}$-specific, $Gag_{241-249}$-specific, or $Gag_{367-381}$-specific stimulation. Intracellular IFN-γ staining was performed with a CytofixCytoperm kit (BD, Tokyo, Japan) and fluorescein isothiocyanate-conjugated anti-human CD4 (BD), peridinin chlorophyll protein-conjugated anti-human CD8 (BD), allophycocyanin (APC)-Cy7-conjugated anti-human CD3 (BD), and phycoerythrin (PE)-conjugated anti-human IFN-γ (Biolegend, San Diego, CA) monoclonal antibodies. Specific T-cell levels were calculated by subtracting nonspecific IFN-γ T-cell frequencies from those after peptide-specific stimulation. Specific T-cell levels lower than 100 per million PBMCs were considered negative.

Sequencing of the viral genome. Plasma RNA was extracted using the High Pure viral RNA kit (Roche Diagnostics, Tokyo, Japan). Fragments corresponding to nucleotides from 1231 to 2958 (containing the entire *gag* region) in the SIVmac239 genome (GenBank accession number M33262) were amplified by nested reverse transcription (RT)-PCR. The PCR products were sequenced using dye terminator chemistry and an automated DNA sequencer (Applied Biosystems, Tokyo, Japan).

Statistical analysis. Statistical analyses were performed using R software (R Development Core Team). Differences in geometric means of plasma viral loads were examined by one-way analysis of variance (ANOVA) and Tukey-Kramer's multiple-comparison test. Plasma viral loads at week 3 were examined for differences between group III and groups II and IV by analysis of covariance (ANCOVA) with week 5 viral loads as a covariate.

RESULTS

CTL responses after prophylactic vaccination. We previously reported the efficacy of vaccination eliciting whole Gag-specific or single $Gag_{241-249}$ epitope-specific CTL memory against SIVmac239 challenge (10, 32). In the present study, we examined the efficacy of prophylactic induction of single $Gag_{206-216}$ epitope-specific CTL memory against SIVmac239 challenge and compared the results with those of the previous experiments.

Five Burmese rhesus macaques possessing MHC-I haplotype *90-120-Ia* received a DNA-prime/SeV-boost vaccine eliciting single $Gag_{206-216}$ epitope-specific CTL responses. A plasmid DNA (p$Gag_{202-216}$-EGFP-N1) and an SeV (SeV-$Gag_{202-216}$-EGFP) vector, both expressing an SIVmac239 $Gag_{202-216}$-EGFP fusion pro-

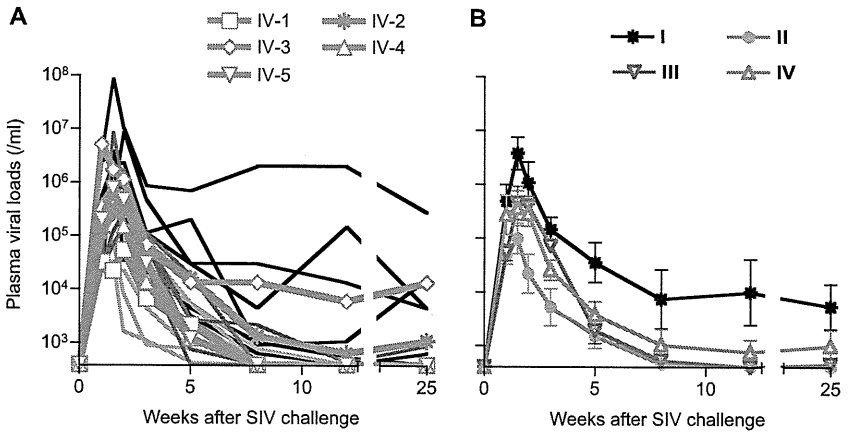

FIG 3 Plasma viral loads after SIVmac239 challenge. The plasma viral loads in group I, group II, group III, and group IV animals were determined as described previously (21). The lower limit of detection was approximately 4×10^2 copies/ml. (A) Changes in plasma viral loads (SIV *gag* RNA copies/ml plasma) after challenge. (B) Changes in geometric means of plasma viral loads after challenge. Groups II and III (but not group IV) showed significantly lower set point viral loads than group I ($P = 0.0390$ between groups I and II, $P = 0.0404$ between groups I and III, and $P > 0.05$ between groups I and IV at week 25 by one-way ANOVA and Tukey-Kramer's multiple-comparison test).

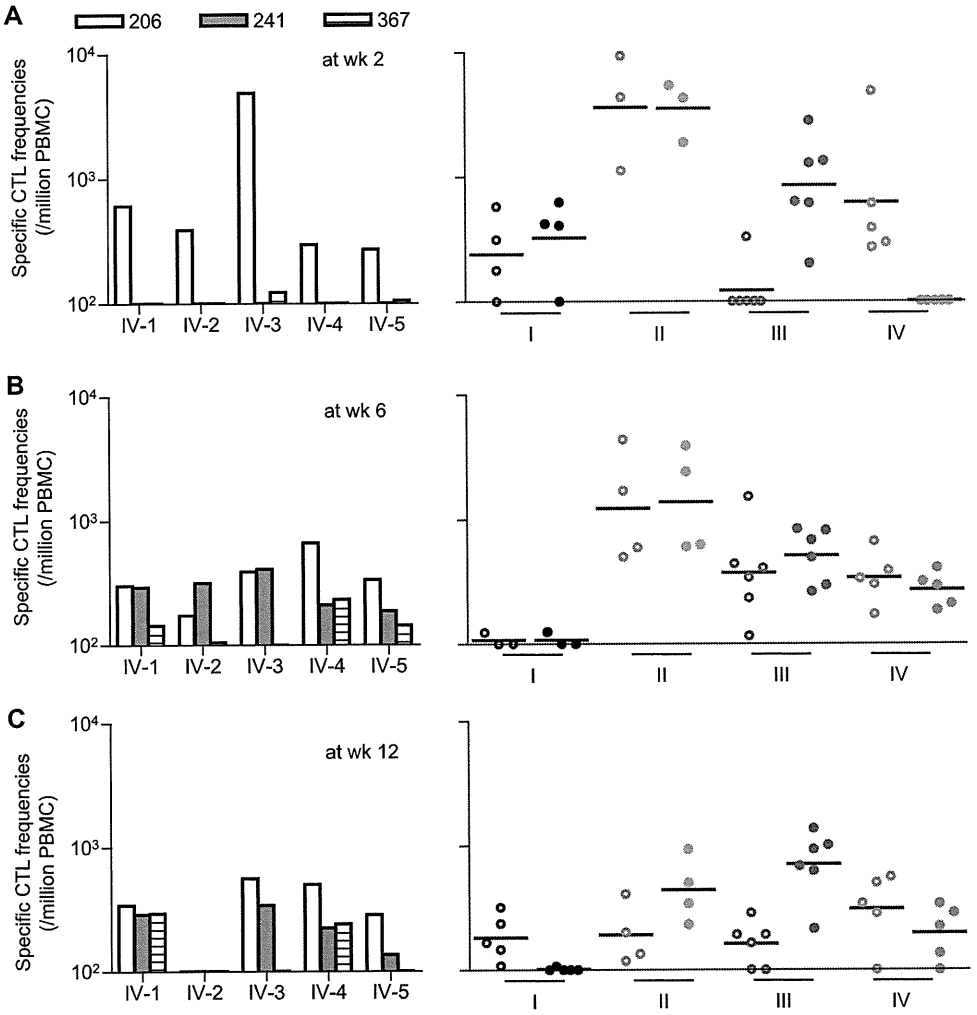

FIG 4 $Gag_{206-216}$-specific and $Gag_{241-249}$-specific CTL responses after SIVmac239 challenge. CTL responses at week 2 (A), week 6 (B), and week 12 (C) are shown. In the graphs on the left, $Gag_{206-216}$-specific (open boxes), $Gag_{241-249}$-specific (closed boxes), and $Gag_{367-381}$-specific (striped boxes) $CD8^+$ T-cell frequencies in group IV macaques are shown. On the right, $Gag_{206-216}$-specific (open circles) and $Gag_{241-249}$-specific (closed circles) $CD8^+$ T-cell frequencies in group I (black), II (green), III (blue), and IV (red) macaques are shown. The bars indicate the geometric mean of each group. Samples from macaques I-1, I-6, II-1, and II-3 at week 2; macaques I-1, I-2, I-6, and II-5 at week 6; and macaques I-1 and II-5 at week 12 were unavailable for this analysis. Statistical analyses among four groups at week 12 revealed significant differences in $Gag_{241-249}$-specific CTL levels (I and III, $P < 0.0001$; I and II, and III and IV, $P < 0.01$; I and IV, II and III, and II and IV, $P > 0.05$ by one-way ANOVA and Tukey-Kramer's multiple-comparison test) but not in $Gag_{206-216}$-specific CTL levels ($P > 0.05$ by one-way ANOVA).

tein, were used for the vaccination (Fig. 1). We confirmed $Gag_{206-216}$-specific CTL responses 1 week after SeV-$Gag_{202-216}$-EGFP boost in all five animals (Fig. 2A). As expected, no $Gag_{241-249}$-specific CTL responses were detected in these animals. No $Gag_{202-216}$-specific $CD4^+$ T-cell responses were detected in the animals except for one (IV-5) showing marginal levels of responses (data not shown).

Plasma viral loads after SIV challenge. We compared these five animals (referred to as group IV) with other groups (I, II, and III) of *90-120-Ia*-positive macaques reported previously (Table 1). Group I animals ($n = 6$) received no vaccination, group II ($n = 5$) received a DNA-prime/SeV-boost vaccine eliciting whole Gag-specific CTL responses, and group III ($n = 6$) received a DNA-prime/SeV-boost vaccine eliciting single $Gag_{241-249}$ epitope-specific CTL responses. Both $Gag_{206-216}$-specific and $Gag_{241-249}$-specific CTL responses were detectable after SeV-Gag boost in four of five group II animals except for one animal (II-3), in which $Gag_{206-216}$-specific, but not $Gag_{241-249}$-specific, CTL responses were detected. In all group III animals, $Gag_{241-249}$-specific CTL responses were confirmed, while no $Gag_{206-216}$-specific CTL responses were detected after SeV-$Gag_{236-250}$-EGFP boost (Fig. 2B).

After SIVmac239 challenge, all animals were infected and showed plasma viremia during the acute phase. Plasma viremia was maintained in five of six unvaccinated animals in group I but became undetectable in one animal (I-2) at week 12. In contrast, all animals in groups II and III contained SIV replication with significantly reduced plasma viral loads compared to group I at the set point. In group IV, however, vaccine efficacy was not so clear; while three out of five animals contained SIV replication, the remaining two (IV-2 and IV-3) failed to control viral replication with persistent plasma viremia (Fig. 3).

Gag-specific CTL responses after SIV challenge. We then measured $Gag_{206-216}$-specific and $Gag_{241-249}$-specific CTL responses after SIVmac239 challenge by detection of peptide-

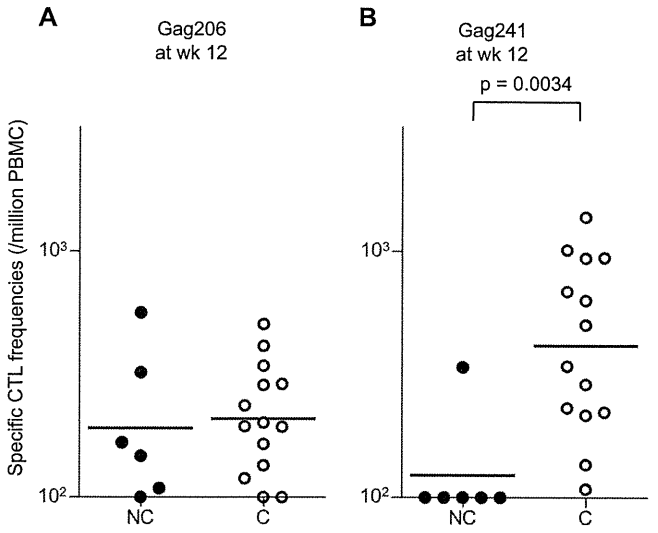

FIG 5 Comparison of $Gag_{206-216}$-specific or $Gag_{241-249}$-specific CTL responses in noncontrollers and controllers at week 12. (A) $Gag_{206-216}$-specific $CD8^+$ T-cell frequencies in noncontrollers (NC; closed circles) and controllers (C; open circles). (B) $Gag_{241-249}$-specific $CD8^+$ T-cell frequencies in noncontrollers and controllers. $Gag_{241-249}$-specific CTL levels in controllers were significantly higher than those in noncontrollers ($P = 0.0034$ by Mann-Whitney test). The bars indicate the geometric mean of each group. Data on a noncontroller (I-1) and a controller (II-5) were unavailable.

specific IFN-γ induction. At week 2 (Fig. 4A), most animals in groups I and II elicited both $Gag_{206-216}$-specific and $Gag_{241-249}$-specific CTL responses, whereas group III animals induced $Gag_{241-249}$-specific CTL responses dominantly. Remarkably, all animals in group IV showed efficient $Gag_{206-216}$-specific CTL responses without detectable $Gag_{241-249}$-specific CTL responses at week 2. These results indicate dominant $Gag_{206-216}$-specific CTL responses with delayed induction of $Gag_{241-249}$-specific CTL responses postchallenge in group IV animals with prophylactic $Gag_{206-216}$-specific CTL induction, and vice versa in group III animals.

At week 6 (Fig. 4B), efficient $Gag_{206-216}$-specific and $Gag_{241-249}$-specific CTL responses were observed in all vaccinated animals in groups II, III, and IV, but not in group I. $Gag_{206-216}$-specific and $Gag_{241-249}$-specific CTL responses were induced equivalently even in groups III and IV. We also examined subdominant $Gag_{367-381}$ epitope-specific CTL responses, which were undetectable at week 2 but became detectable at week 6 in most group IV animals (Fig. 4, graphs on left). At week 12 (Fig. 4C), however, different CTL immunodominance patterns were observed among the groups. $Gag_{241-249}$-specific CTL levels were higher than $Gag_{206-216}$-specific levels in groups II and III but were reduced in groups I and IV. Interestingly, comparison between the animals with persistent viremia (referred to as noncontrollers) and those controlling SIV replication (referred to as controllers) revealed significant differences in $Gag_{241-249}$-specific CTL levels, but not in $Gag_{206-216}$-specific levels, at week 12 ($P = 0.0034$ by Mann-Whitney test) (Fig. 5).

Selection of a CTL escape mutation. Next, we examined viral genome *gag* sequences at weeks 5 and 12 after challenge to determine whether CTL escape mutations were selected in these animals (Table 2). At week 5, a mutation leading to an L-to-S substitution at the 216th residue in Gag (L216S) was selected in all the group II animals. This GagL216S change results in escape from $Gag_{206-216}$-specific CTL recognition, as described previously (21). All the group IV animals with $Gag_{206-216}$-specific CTL induction also showed rapid selection of this CTL escape mutation at week 5. Analysis at week 3 found the GagL216S mutation dominant in two (II-2 and II-5) group II and two (IV-1 and IV-3) group IV animals (data not shown). However, animals in group III showed no *gag* mutations at week 5, except for one animal (III-5) selecting a mutation leading to an L-to-F substitution at the 216th residue. Later, at week 12, the $Gag_{206-216}$-specific CTL escape mutation, GagL216S, was selected even in group III animals. No animals showed mutations around the $Gag_{241-249}$ epitope-coding region even at week 12. These results indicate that selection of this $Gag_{206-216}$-specific CTL escape mutation may be accelerated by prophylactic vaccination inducing $Gag_{206-216}$-specific CTL responses. On the other hand, in group III animals with single $Gag_{241-249}$ epitope-specific CTL induction, selection of a $Gag_{206-216}$-specific CTL escape mutation was delayed but was observed before selection of a $Gag_{241-249}$-specific CTL escape mutation, suggesting strong selective pressure by delayed $Gag_{206-216}$-specific CTL responses after SIV challenge.

In order to see the effect of rapid selection of the $Gag_{206-216}$-specific CTL escape mutation on SIV control, we compared plasma viral loads at weeks 3 and 5 between groups II and IV (referred to as group II+IV) with rapid selection of the GagL216S

TABLE 2 Selection of a CTL escape mutation

Group	Macaque ID	Amino acid change for Gag residues[b]: 206–216		241–249	
		Wk 5	Wk 12	Wk 5	Wk 12
I	I-1	None	ND	None	ND
	I-2[a]	None	L216S	None	None
	I-3	None	L216S	None	None
	I-4	None	None	None	None
	I-5	None	None	None	None
	I-6	None	None	None	None
II	II-1[a]	L216S	ND	None	ND
	II-2[a]	L216S	ND	None	ND
	II-3[a]	L216S	ND	None	ND
	II-4[a]	L216S	ND	None	ND
	II-5[a]	L216S	ND	None	ND
III	III-1[a]	None	L216S	None	None
	III-2[a]	None	L216S	None	None
	III-3[a]	None	NA	None	NA
	III-4[a]	None	NA	None	NA
	III-5[a]	L216F	L216S	None	None
	III-6[a]	None	L216S	None	None
IV	IV-1[a]	L216S	L216S	None	None
	IV-2	L216S	L216S	None	None
	IV-3	L216S	L216S	None	None
	IV-4[a]	L216S	L216S	None	None
	IV-5[a]	L216S	NA	None	NA

[a] Animals that controlled SIV replication at week 12 (controllers).
[b] Plasma viral gag genome mutations were examined at weeks 5 and 12. Amino acid substitutions in $Gag_{206-216}$ and $Gag_{241-249}$ epitope regions are shown. L216S results in viral escape from $Gag_{206-216}$-specific CTL recognition. It remains undetermined whether L216F results in CTL escape. ND, not determined; NA, not determined because Gag fragments were unable to be amplified from plasma RNA.

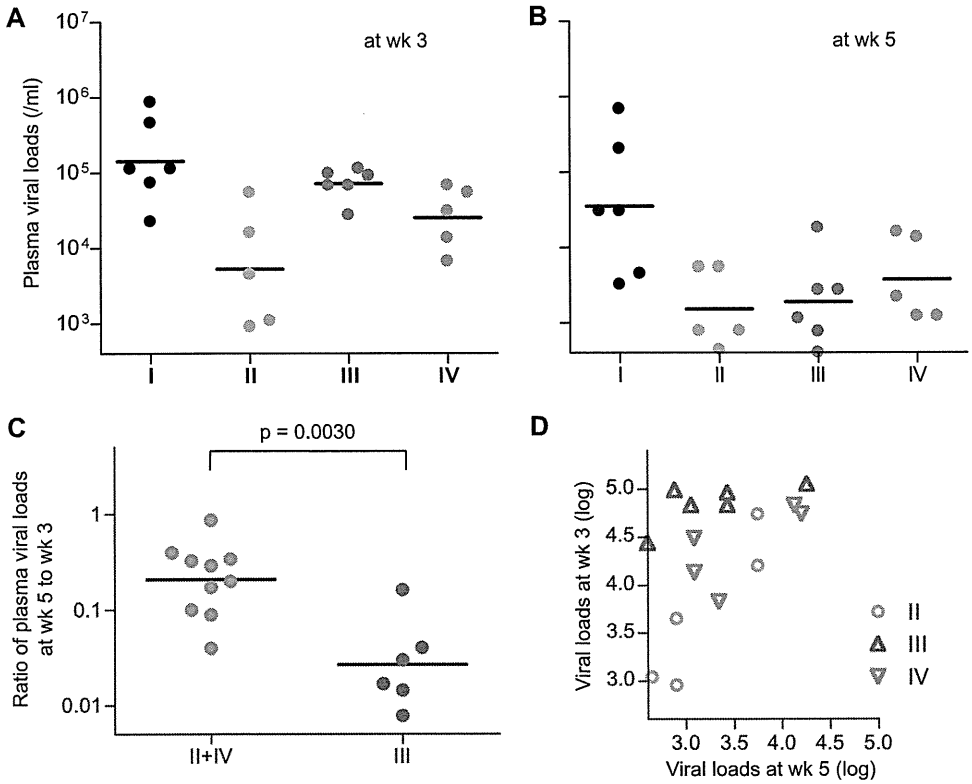

FIG 6 Comparison of plasma viral loads at weeks 3 and 5 among four groups. (A) Plasma viral loads at week 3 in group I, II, III, and IV animals. (B) Plasma viral loads at week 5 in group I, II, III, and IV animals. (C) Comparison of ratios of plasma viral loads at week 5 to week 3 in group II+IV animals and group III animals. The ratios in group III were significantly lower than those in group II+IV ($P = 0.0030$ by Mann-Whitney test). The bars indicate the geometric mean of each group. (D) Scatter plots between plasma viral loads at weeks 3 and 5 in group II, III, and IV animals.

mutation and group III without the mutation at week 5 (Fig. 6). Ratios of plasma viral loads at week 5 to week 3 in group III were significantly lower than those in group II+IV ($P = 0.0030$ by Mann-Whitney test) (Fig. 6C). To confirm this result, we examined the difference in week 3 viral loads between groups III and II+IV by ANCOVA, with week 5 viral loads as a covariate. This analysis revealed that week 3 viral loads controlled for by week 5 viral loads were significantly higher in group III than those in group II+IV (Fig. 6D and Table 3); i.e., the decline in viral loads from week 3 to week 5 was significantly sharper in group III than in group II+IV, possibly reflecting viral escape from suppressive pressure by $Gag_{206-216}$-specific CTL responses in the latter group during this period (from week 3 to week 5).

DISCUSSION

In the present study, we analyzed the impact of vaccination inducing single $Gag_{206-216}$ epitope-specific CTL memory on postchallenge CTL responses and SIV control in *90-120-Ia*-positive macaques and then compared the results with those of vaccination inducing single $Gag_{241-249}$ epitope-specific CTL responses. Our results indicate that these prophylactic vaccinations result in different patterns of $Gag_{206-216}$-specific and $Gag_{241-249}$-specific CTL immunodominance and cooperation after SIVmac239 challenge.

Unvaccinated *90-120-Ia*-positive macaques (group I) showed both $Gag_{206-216}$-specific and $Gag_{241-249}$-specific CTL responses after SIV challenge. In group IV animals with prophylactic induc-

TABLE 3 ANCOVA on week 3 viral loads with week 5 viral loads as a covariate between groups III and II+IV

ANOVA	Parameter	SS[a]	df[b]	MS[c]	*F*	*P* value
Homogeneity of slopes of regression	Group × slope	0.304	1	0.304	2.099	0.173
	Residual	1.735	12	0.145		
	Total	2.038	13	0.157		
Difference in week 3 viral loads with week 5 viral loads as a covariate between groups III and II+IV	Effect and group	1.106	1	1.106	7.052	0.020
	Residual	2.038	13	0.157		
	Total	3.144	14	0.225		

[a] SS, sum of squares.
[b] df, degrees of freedom.
[c] MS, mean squares.